

Supersymmetric Seesaw without Singlet Neutrinos: Neutrino Masses and Lepton-Flavour Violation

Anna Rossi

*Dipartimento di Fisica ‘G. Galilei’, Università di Padova and
INFN, Sezione di Padova, Via Marzolo 8, I-35131 Padua, Italy*
E-mail address: arossi@pd.infn.it

Abstract

We consider the supersymmetric seesaw mechanism induced by the exchange of heavy $SU(2)_W$ triplet states, rather than ‘right-handed’ neutrino singlets, to generate neutrino masses. We show that in this scenario the neutrino flavour structure tested at low-energy in the atmospheric and solar neutrino experiments is directly inherited from the neutrino Yukawa couplings to the triplets. This allows us to predict the ratio of the $\tau \rightarrow \mu\gamma$ (or $\tau \rightarrow e\gamma$) and $\mu \rightarrow e\gamma$ decay rates in terms of the low-energy neutrino parameters. Moreover, once the model is embedded in a grand unified model, quark-flavour violation can be linked to lepton-flavour violation.

1 Introduction

Nowadays we have one more important piece of information concerning the flavour structure of the Standard Model: flavour violation is also present in the lepton sector. So far this has only shown up in the atmospheric and solar neutrino experiments [1, 2]. The anomalies observed in these experiments can be interpreted in terms of neutrino oscillations which are the result of non-vanishing neutrino masses and mixing angles [3, 4]. In the framework of the Standard Model (or of its supersymmetrized version) the latter properties effectively arise from the following lepton-number (L) violating $d = 5$ operator [5]:

$$\frac{1}{2M_L} \mathbf{Y}_\nu^{ij} (L_i H_2)(L_j H_2), \quad \mathbf{Y}_\nu = \mathbf{Y}_\nu^T \quad (1)$$

where $i, j = 1, 2, 3$ are family indices, M_L is the energy scale where L is broken, L_i are the $SU(2)_W$ lepton doublets and H_2 is the Higgs doublet with hypercharge $Y = 1/2$. Upon breaking $SU(2)_W \times U(1)_Y$ by the vacuum expectation value of the Higgs field, $\langle H_2 \rangle = v_2 = v \sin \beta$ ($v = 174 \text{ GeV}$), the operator (1) induces Majorana masses for the neutrinos,

$$\mathbf{m}_\nu^{ij} = \frac{v_2^2}{M_L} \mathbf{Y}_\nu^{ij}. \quad (2)$$

Therefore, from here we can easily understand the origin of the tiny neutrino masses, as they may be suppressed by some large scale M_L . Taking for instance a neutrino mass $m_\nu \sim (10^{-1} - 10^{-2}) \text{ eV}$ as indicated by the atmospheric neutrino data (and assuming a hierarchical neutrino spectrum) [6], the magnitude of M_L can be inferred,

$$Y_\nu^{-1} M_L \sim 10^{15} \text{ GeV}. \quad (3)$$

In the basis in which the charged-lepton Yukawa matrix \mathbf{Y}_e is diagonal, all the lepton-flavour violation is contained in the coupling matrix \mathbf{Y}_ν , i.e. in the neutrino mass matrix:

$$\mathbf{m}_\nu = \mathbf{U}^\star \mathbf{m}_\nu^D \mathbf{U}^\dagger, \quad \mathbf{m}_\nu^D = \text{diag}(m_1, m_2, m_3) \quad (4)$$

where m_1, m_2, m_3 are the neutrino mass eigenvalues, and the unitary matrix \mathbf{U} is the lepton mixing matrix that appears in the charged lepton current $\bar{\ell} \gamma^\mu (1 - \gamma_5) \mathbf{U} \nu$ and is responsible for neutrino oscillations.

In principle lepton-flavour violation could also be tested in other processes, such as $\mu \rightarrow e\gamma$, $\tau \rightarrow \mu\gamma$ and $\tau \rightarrow e\gamma$. The present experimental limits on these decays are [7]:

$$\begin{aligned} BR(\mu \rightarrow e\gamma) &< 1.2 \times 10^{-11}, \\ BR(\tau \rightarrow \mu\gamma) &< 1.1 \times 10^{-6}, \\ BR(\tau \rightarrow e\gamma) &< 2.7 \times 10^{-6}, \end{aligned} \quad (5)$$

which could be significantly improved, the first down to 10^{-14} [8] and the second to 10^{-9} [9]. In the Standard Model it is very hard to obtain interesting results because the decay amplitudes are strongly GIM-suppressed by the tiny neutrino masses, $m_i \ll M_W$ [10]. On

the other hand, in the framework of the minimal supersymmetric extension of the Standard Model (MSSM), those processes can be enhanced through the one-loop exchange of superpartners, if the masses of the latter are not too heavy and do not conserve flavour [11]. Concerning the latter property, we could expect that the underlying flavour theory dictates both the flavour structure of the standard fermion mass matrices and that of the corresponding supersymmetric scalar partners (see e.g. [12]). Even if sfermion masses are universal (i.e. flavour-blind) at high energy, as in minimal supergravity or gauge mediated supersymmetry breaking scenarios, nevertheless flavour conservation can be broken in the sfermion masses by radiative effects due to flavour-violating Yukawa couplings [13, 14]. In particular, the interactions that generate the operator (1) also induce lepton-flavour violation (LFV) in the slepton mass matrices by renormalization effects. A well-known and investigated example is that of the standard seesaw mechanism [15] in which LFV is induced radiatively by Yukawa couplings of the $SU(2)_W$ -doublet neutrinos with singlet neutrinos N (often referred to as right-handed neutrinos) [13, 16]. Here, we would like to discuss another example of seesaw scenario in which the $d = 5$ operator (1) is obtained by exchanging heavy $SU(2)_W$ triplets with non-zero hypercharge. We recall that models with scalar triplets to generate Majorana neutrino masses have been considered in the literature for a long time, though they have received less attention than the standard seesaw scenario. For example, a model with spontaneous L -breaking was proposed in [17] and later on extended [18]. A triplet-exchange seesaw realization with explicit L -breaking was also introduced [19], in a non-supersymmetric framework¹. A supersymmetric version of the latter scenario was recently introduced to have baryogenesis through leptogenesis [22]. In this work we shall further elaborate the supersymmetric triplet seesaw scenario. In particular, we shall discuss how LFV is radiatively induced in the slepton masses and show that this scenario is potentially more predictive than the N -induced seesaw one.

This paper is organised as follows. In Sect. 2 we review both the standard seesaw mechanism and that in which triplet states are exchanged. This presentation will help in showing the differences between the two scenarios and outline the one-to-one correspondence between the neutrino parameters and LFV in the soft-breaking parameters that characterizes the triplet seesaw scenario. In Sect. 3 the triplet seesaw is embedded in $SU(5)$ context. In Sect. 4 we show the general pattern of \mathbf{Y}_ν as derived from the low-energy neutrino data. In Sect. 5 we discuss the flavour-violation induced in the soft-breaking terms by radiative effects in the energy range above the triplet mass threshold. The renormalization group equations (RGEs) relevant to our study are confined in Appendix. In Sect. 6, after giving the qualitative behaviour of the $\ell_i \rightarrow \ell_j \gamma$ branching ratios, we also discuss some numerical examples. We give our conclusions in Sect. 7.

¹ Recently, this scenario was studied for leptogenesis [20]. An alternative seesaw mechanism, obtained by exchanging heavy $SU(2)_W$ triplets with zero hypercharge, was discussed in [21].

2 Singlet versus Triplet seesaw

First, we briefly review the standard seesaw mechanism in which singlet states N are exchanged [15]. The relevant superpotential terms at the scale where lepton number is broken are:

$$\mathbf{Y}_N^{ij} N_i L_j H_2 + \frac{1}{2} \mathbf{M}_N^{ij} N_i N_j, \quad (6)$$

where $i, j = 1, 2, 3$ are family indices, \mathbf{Y}_N is an arbitrary 3×3 matrix of Dirac-like Yukawa couplings, while \mathbf{M}_N is a 3×3 symmetric mass matrix describing Majorana masses for the singlets N . If the N states are assigned lepton number $L = -1$, the second term in (6) explicitly breaks L . After decoupling the heavy states N at the (overall) scale M_L , the lepton-number violating $d = 5$ operator (1) is generated, where $M_L^{-1} \mathbf{Y}_\nu$ is identified as follows:

$$\frac{1}{M_L} \mathbf{Y}_\nu^{ij} = \mathbf{Y}_N^{Tik} \mathbf{M}_N^{-1kl} \mathbf{Y}_N^{lj}. \quad (7)$$

Finally, at the electroweak scale Majorana masses for the neutrinos are obtained,

$$\mathbf{m}_\nu^{ij} = \frac{v_2^2}{M_L} \mathbf{Y}_\nu^{ij} = v_2^2 \mathbf{Y}_N^{Tik} \mathbf{M}_N^{-1kl} \mathbf{Y}_N^{lj}. \quad (8)$$

As a matter of fact, there is a certain degree of ambiguity in the effective neutrino mass matrix: its flavour structure reflects both that of the arbitrary Dirac-like matrix \mathbf{Y}_N and that of the matrix \mathbf{M}_N . From a bottom-up perspective, this implies that neutrino masses and mixing angles, inferred by the low-energy neutrino data [6], may only reflect the *effective* Yukawa matrix \mathbf{Y}_ν and the overall mass scale M_L (modulo radiative corrections) but cannot be unambiguously related to the more fundamental quantities, \mathbf{Y}_N and \mathbf{M}_N (for a recent discussion on this aspect see for example [23] and references therein). In other words, the low-energy parameters, described by \mathbf{Y}_ν , which amount to 6 real parameters + 3 phases, are less than the number of the independent ‘fundamental’ physical parameters in \mathbf{Y}_N and \mathbf{M}_N , which instead are 12 real parameters + 6 phases.

Now, let us consider the triplet seesaw scenario. The relevant superpotential terms are

$$\frac{1}{\sqrt{2}} \mathbf{Y}_T^{ij} L_i T L_j + \frac{1}{\sqrt{2}} \lambda_1 H_1 T H_1 + \frac{1}{\sqrt{2}} \lambda_2 H_2 \bar{T} H_2 + M_T T \bar{T} + \mu H_1 H_2, \quad (9)$$

where the super-multiplets T, \bar{T} are in a vector-like $SU(2)_W \times U(1)_Y$ representation², $T \sim (3, 1)$ and $\bar{T} \sim (3, -1)$, and H_1 is the Higgs doublet with hypercharge $Y = -1/2$. The matrix \mathbf{Y}_T^{ij} is in general a 3×3 symmetric matrix, $\mathbf{Y}_T^{ij} = \mathbf{Y}_T^{ji}$. If we assign lepton number $L = -2$ (2) to the triplet T (\bar{T}), we can see that the λ_1, λ_2 -couplings explicitly break L . If instead we assign $L = -2$ to T and $L = 0$ to \bar{T} , then the L -breaking parameters are M_T and λ_1 . In eq. (9) the triplets T, \bar{T} are represented as 2×2 matrices, namely

$$T = (i\sigma_2) \mathbf{T} \cdot \boldsymbol{\sigma} = \begin{pmatrix} T^0 & -\frac{1}{\sqrt{2}} T^+ \\ -\frac{1}{\sqrt{2}} T^+ & -T^{++} \end{pmatrix}, \quad \bar{T} = (i\sigma_2) \bar{\mathbf{T}} \cdot \boldsymbol{\sigma} = \begin{pmatrix} \bar{T}^{--} & -\frac{1}{\sqrt{2}} \bar{T}^- \\ -\frac{1}{\sqrt{2}} \bar{T}^- & -\bar{T}^0 \end{pmatrix}, \quad (10)$$

²Notice that in the supersymmetric picture two triplets, T and \bar{T} , are required.

where the matrices σ_a ($a = 1, 2, 3$) are the Pauli matrices and the components T_1, T_2, T_3 and $\bar{T}_1, \bar{T}_2, \bar{T}_3$ of \mathbf{T} and $\bar{\mathbf{T}}$, respectively, can be easily inferred³. By decoupling the triplet states at the scale M_T we again obtain the $d = 5$ effective operator of eq. (1). Now, however, the flavour structure of the matrix \mathbf{Y}_ν is *the same* as that of \mathbf{Y}_T , that is:

$$\frac{1}{M_L} \mathbf{Y}_\nu^{ij} = \frac{\lambda_2}{M_T} \mathbf{Y}_T^{ij}, \quad (11)$$

and the Majorana neutrino mass matrix is given by:

$$\mathbf{m}_\nu^{ij} = \frac{v_2^2}{M_L} \mathbf{Y}_\nu^{ij} = \frac{v_2^2 \lambda_2}{M_T} \mathbf{Y}_T^{ij}. \quad (12)$$

Fig. 1 shows the diagrams inducing the supersymmetric $d = 5$ operator (1) in the N -seesaw (a) and T -seesaw (b). In terms of component fields, the neutrino mass operator is generated through the exchange of the N fermion component in the former realization, while in the latter realization it is generated by the exchange of the T scalar component and of the \bar{T} F-component which gives rise to the effective scalar coupling $\lambda_2 M_T H_2 T^\dagger H_2$. This latter feature also allows us to appreciate the supersymmetric version (9) of the T -induced seesaw. In the non-supersymmetric case [19] the coefficient of the cubic interaction $HT^\dagger H$ is an independent mass parameter, say Λ , and therefore $\mathbf{m}_\nu = v^2 \frac{\Lambda}{M_T^2} \mathbf{Y}_T$.

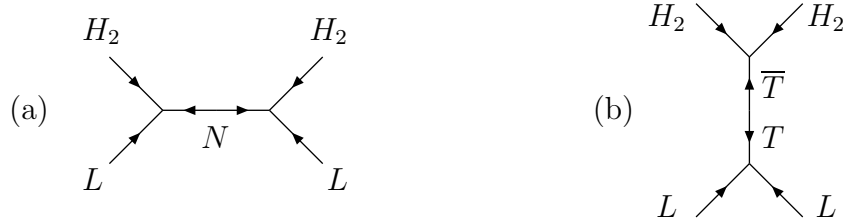


Figure 1: Contributions to the LLH_2H_2 effective operator: (a) heavy singlet exchange; (b) heavy triplet exchange.

The difference with the standard N -induced seesaw case is manifest: in the T -seesaw scenario the neutrino mass matrix can be *directly* related to the fundamental \mathbf{Y}_T matrix and to one relevant mass scale parameter, M_T/λ_2 . In particular, the amount of lepton-flavour violation measured at low-energy through the lepton mixing can directly be linked to the only source of lepton-flavour violation, the Yukawa matrix \mathbf{Y}_T given at the scale M_T . The counting of the independent parameters reveals indeed that in this model the independent \mathbf{Y}_T parameters, 6 real parameters + 3 phases, are just matched by the low-energy physical parameters. There are left other 2 real parameters, M_T and λ_2 , whose ratio is directly involved in the neutrino mass generation, plus λ_1 which in general is complex and is not directly connected to the neutrino parameters. In summary: while in the N -induced seesaw

³ As a consequence of the representation adopted for T and \bar{T} (10), the $SU(2)_W$ -invariant mass term in eq. (9) is to be understood as $M_T T \bar{T} = M_T \text{Tr}(T i \sigma_2 \bar{T} i \sigma_2)$.

scenario there are two lepton-flavour violation sources, the matrices \mathbf{Y}_N and \mathbf{M}_N , in the T -induced seesaw scenario the matrix \mathbf{Y}_T is the only source of lepton-flavour violation⁴.

The implications of all this are even more dramatic when we consider the lepton-flavour violation induced through renormalization effects. Since a long it has been pointed out that the Yukawa couplings \mathbf{Y}_N in eq. (6) can induce non-vanishing lepton-flavour violating entries in the mass matrices of the left-handed sleptons through radiative corrections [13], even in the minimal SUSY scenario with universal soft-breaking terms at the GUT scale M_G , $m_{\tilde{L}}^2 = m_{\tilde{e}}^2 = \dots = m_0^2 \mathbb{1}$. The form of the LFV entries is

$$(\mathbf{m}_{\tilde{L}}^2)_{ij} \propto m_0^2 (\mathbf{Y}_N^\dagger \mathbf{Y}_N)_{ij} \log \frac{M_G}{M_N}, \quad i \neq j. \quad (13)$$

In this scenario, according to our previous discussion, the size of LFV cannot be unambiguously predicted in a bottom-up approach making use of the low-energy data⁵.

Now let us see what can occur in the T -seesaw scenario. In this case, the lepton-flavour violating entries are *directly* connected to the effective neutrino mass matrices, as

$$(\mathbf{m}_{\tilde{L}}^2)_{ij} \propto m_0^2 (\mathbf{Y}_T^\dagger \mathbf{Y}_T)_{ij} \log \frac{M_G}{M_T}, \quad i \neq j, \quad (14)$$

or more explicitly,

$$(\mathbf{m}_{\tilde{L}}^2)_{ij} \propto m_0^2 \left(\frac{M_T}{\lambda_2 v_2^2} \right)^2 (\mathbf{m}_\nu^\dagger \mathbf{m}_\nu)_{ij} \log \frac{M_G}{M_T} \sim m_0^2 \left(\frac{M_T}{\lambda_2 v_2^2} \right)^2 [\mathbf{U}(\mathbf{m}_\nu^D)^2 \mathbf{U}^\dagger]_{ij} \log \frac{M_G}{M_T}. \quad (15)$$

This expression enables us to *univocally* predict the ratio of the lepton-flavour violation in the 2-3 sector with that in the 1-2 sector, essentially in terms of the low-energy parameters, namely:

$$\frac{(m_{\tilde{L}}^2)_{\tau\mu}}{(m_{\tilde{L}}^2)_{\mu e}} \approx \frac{[\mathbf{U}(\mathbf{m}_\nu^D)^2 \mathbf{U}^\dagger]_{\tau\mu}}{[\mathbf{U}(\mathbf{m}_\nu^D)^2 \mathbf{U}^\dagger]_{\mu e}}, \quad (16)$$

or for the 1-3 sector

$$\frac{(m_{\tilde{L}}^2)_{\tau e}}{(m_{\tilde{L}}^2)_{\mu e}} \approx \frac{[\mathbf{U}(\mathbf{m}_\nu^D)^2 \mathbf{U}^\dagger]_{\tau e}}{[\mathbf{U}(\mathbf{m}_\nu^D)^2 \mathbf{U}^\dagger]_{\mu e}}. \quad (17)$$

Thus we can relate the rate of the $\tau \rightarrow \mu\gamma$ or $\tau \rightarrow e\gamma$ decay with that of the $\mu \rightarrow e\gamma$ decay. This is the main feature of our discussion.

⁴ Notice that in this seesaw scenario one triplet pair T, \bar{T} is enough to generate non-vanishing mass for all three neutrinos, whilst in the standard seesaw three singlets N are necessary for that. Also notice that, from the flavour point of view, the seesaw realized by exchanging hyperchargeless triplets $T' \sim (3, 0)$ [21] is more similar to the N -induced seesaw. Indeed: i) such triplets T' are exchanged in the same channel as the singlets N (see Fig. 1 (a)); ii) three hyperchargeless triplets are required to give mass to all three neutrinos; iii) two sources of flavour-dependence appear, the matrix $Y_{T'}$ in the Yukawa interaction $\mathbf{Y}_T L T' H_2$, and the mass matrix $\mathbf{M}_{T'}$ of the triplets.

⁵The authors of [23] indeed regard the combination $\mathbf{Y}_N^\dagger \mathbf{Y}_N$, responsible for the LFV in the slepton masses, as a further ‘observable’ which provides the lacking 6 real parameters + 3 phases necessary to fully determine both \mathbf{Y}_N and \mathbf{M}_N .

This scenario is susceptible of being further elaborated. Indeed, the presence of the extra $SU(2)_W$ -triplet states T, \bar{T} at intermediate energy would spoil the gauge coupling unification which takes place with the field content of the MSSM. A simple way to save gauge coupling unification is to introduce more states X , to complete a certain representation R – such that $R = T + X$ – of some unifying gauge group G , $G \supset SU(3) \times SU(2)_W \times U(1)_Y$. Thus we can envisage three (minimal) scenarios:

- (A)- The states X , though with mass $M_X \sim M_T$, are assumed to have vanishing or negligible interactions with the other states, except for the gauge interactions. This may be the case either if we prefer not to embed the theory in any definite grand unified theory (GUT) or if we embed it in some GUT and the Yukawa interactions of the states T and X have different strength due to GUT breaking effects. In particular, we could have negligible Yukawa coupling for the fragments X and, on the contrary, non-vanishing Yukawa coupling for the fragments T .
- (B)- The theory is embedded in a GUT but, contrary to the ansatz (A), the Yukawa couplings of the states X are assumed to be non-vanishing and related to those of the triplet partners T . Indeed, this is generally the case in minimal GUT models. In this case we will generate not only lepton- flavour violation but also closely related flavour violation in the quark sector (related to the X -couplings).
- (C)- There are no extra states X or, equivalently, they are considered to be split in mass from the triplets T and be decoupled at a scale $\mu \geq M_G$. In this case, the simple unification of gauge couplings is lost and large threshold corrections are needed to recover it.

3 SUSY $SU(5)$ scenario with $SU(2)_W$ triplets

As already mentioned in the previous section, the extra states T, \bar{T} with mass M_T much below the GUT scale would destroy the gauge coupling unification. In principle the latter property could be recovered at the price of invoking large threshold corrections. In the next, however, we prefer to maintain the simple gauge coupling unification. To this purpose, the field content of the model can be minimally extended by adding the other components of the $SU(5)$ representations, 15 and $\bar{15}$, in which the triplets T and \bar{T} can indeed fit. In terms of $SU(3) \times SU(2)_W \times U(1)_Y$ representations, the 15 -multiplet decomposes as follows:

$$15 = S + T + Z, \\ S \sim (6, 1, -\frac{2}{3}), \quad T \sim (1, 3, 1), \quad Z \sim (3, 2, \frac{1}{6}), \quad (18)$$

(the $\bar{15}$ -decomposition is obvious). The presence of these extra states fitting a complete GUT multiplet changes the value of the gauge coupling α_G at the GUT scale, with respect to the MSSM case, but does not modify the value of the unification scale M_G (to one loop

accuracy). The β -functions of the gauge couplings in the RGEs get modified as follows ($a = 1, 2, 3$):

$$\begin{aligned}
16\pi^2 \frac{dg_a}{dt} &= B_a g_a^3, \\
B_1 &= b_1 + \frac{3}{5} \left(\frac{8}{3} n_S + 3n_T + \frac{1}{6} n_Z \right) = b_1 + \frac{7}{2} n_{15}, \\
B_2 &= b_2 + 2n_T + \frac{3}{2} n_Z = b_2 + \frac{7}{2} n_{15}, \\
B_3 &= b_3 + \frac{5}{2} n_S + n_Z = b_3 + \frac{7}{2} n_{15},
\end{aligned} \tag{19}$$

where b_a are the coefficients of the β -functions in the MSSM, namely $b_1 = \frac{33}{5}$, $b_2 = 1$, $b_3 = -3$, and we have explicitly shown the contribution of the new states ($n_S = N_S + N_{\bar{S}}$, $n_T = N_T + N_{\bar{T}}$, $n_Z = N_Z + N_{\bar{Z}}$ and $n_{15} = N_{15} + N_{\bar{15}}$ in a self-explanatory notation). As expected, for each B_a the overall contribution of S, T, Z just reproduces the Dynkin index $\frac{7}{2}$ of the $SU(5)$ 15 representation. The enhancement of the β -functions makes the gauge couplings increase faster at higher energy. For instance, by using the low-energy values of α_{em} , α_s and $\sin^2 \theta_W$ and assuming an average SUSY threshold close to the top mass, for T, S, Z masses around 10^{14} GeV we find that at one-loop g_1 and g_2 get unified at $M_G \sim 2 \times 10^{16}$ GeV to the common value $g_G \sim 0.88$, while the value of g_3 differs by one per mill or so. In the MSSM we would find $g_G \sim 0.71$.

The $SU(5)$ invariant superpotential (omitting for simplicity the flavour indices) reads as:

$$\begin{aligned}
W_{SU(5)} &= \frac{1}{\sqrt{2}} \mathbf{Y}_{15\bar{5}} 15 \bar{5} + \frac{1}{\sqrt{2}} \lambda_1 \bar{5}_H 15 \bar{5}_H + \frac{1}{\sqrt{2}} \lambda_2 5_H \bar{15} 5_H + \mathbf{Y}_5 10 \bar{5} \bar{5}_H \\
&\quad + \mathbf{Y}_{10} 10 10 5_H + M_{15} 15 \bar{15} + M_5 \bar{5}_H 5_H,
\end{aligned} \tag{20}$$

where the matter multiplets are understood as $\bar{5} = (d^c, L)$, $10 = (u^c, e^c, Q)$ and the Higgs doublets fit with their coloured partners, t, \bar{t} as $5_H = (t, H_2)$, $\bar{5}_H = (\bar{t}, H_1)$. In the 15-multiplet the states S, T and Z are accommodated as:

$$15^{AB} = \begin{pmatrix} S^{ab} & \frac{1}{\sqrt{2}} Z^{aj} \\ \frac{1}{\sqrt{2}} Z^{bi} & T^{ij} \end{pmatrix} \tag{21}$$

where the $SU(5)$ -indices $A, B = 1, 2, 3, 4, 5$ are decomposed into $SU(3)$ indices $a, b = 1, 2, 3$ and $SU(2)_W$ indices $i, j = 4, 5$, $A = (a, i)$, $B = (b, j)$. In eq. (21) it is understood that $S^{aa} = \hat{S}^{aa}$, $S^{ab} = \frac{1}{\sqrt{2}} \hat{S}^{ab}$ ($a \neq b$) and $T^{ii} = \hat{T}^{ii}$, $T^{ij} = \frac{1}{\sqrt{2}} \hat{T}^{ij}$ ($i \neq j$) (cfr. eq. (10)) where the fields $\hat{S}^{ab}, \hat{T}^{ij}$ are those canonically normalized. It is well-known that the minimal $SU(5)$ model in which the Yukawa matrices $\mathbf{Y}_5, \mathbf{Y}_{10}$ are true constants is not phenomenologically satisfactory. The latter should be rather understood as field dependent quantities, e.g. $\mathbf{Y}_5(\Phi) = \mathbf{Y}_5^{(0)} + \mathbf{Y}_5^{(1)} \Phi/M + \dots$ where Φ is the adjoint 24 of $SU(5)$ and M is some cutoff scale larger than the GUT scale M_G . This perspective allows us to correct certain $SU(5)$ -symmetry relations, such as $\mathbf{Y}_d = \mathbf{Y}_e^T$ [24]. Moreover, some mechanism is also necessary to

split the masses⁶ of the doublet $H_{1,2}$ and triplet t, \bar{t} components of $\bar{5}_H, \bar{5}_H$ not to have fast proton decay mediated by the coloured states t, \bar{t} [25]. We shall therefore adopt this point of view for the whole $SU(5)$ extended model of eq. (20). In the $SU(5)$ -broken phase, beneath M_G , the superpotential reads as:

$$\begin{aligned} & \frac{1}{\sqrt{2}}(\mathbf{Y}_T L T L + \mathbf{Y}_S d^c S d^c) + \mathbf{Y}_Z d^c Z L + \mathbf{Y}_d d^c Q H_1 + \mathbf{Y}_e e^c L H_1 + \mathbf{Y}_u u^c Q H_2 \\ & + \frac{1}{\sqrt{2}}(\lambda_1 H_1 T H_1 + \lambda_2 H_2 \bar{T} H_2) + M_T T \bar{T} + M_Z Z \bar{Z} + M_S S \bar{S} + \mu H_1 H_2. \end{aligned} \quad (22)$$

As already mentioned, the couplings involving the coloured triplets t, \bar{t} do not appear as the latter are assumed to decouple at the GUT scale M_G to suppress dangerous $B - L$ violating $d = 5$ operators. On the contrary, at the decoupling of the 15 fragments, no $B - L$ violating $d = 5$ operators are induced, apart from the ‘neutrino’ operator, since the $\bar{15}$ states do not couple to the matter multiplets $\bar{5}, 10$. Only flavour-conserving $d = 6$ operators are generated, i.e. $(L d^c)(\bar{L} \bar{d}^c)$, $(d^c d^c)(\bar{d}^c \bar{d}^c)$, $(LL)(\bar{L} \bar{L})$ in the Kähler potential, which, being suppressed by the square of the large scale M_{15} , are not relevant for the low-energy phenomenology. Notice that in the minimal case the masses M_T, M_S, M_Z are equal at the GUT scale,

$$M_S = M_T = M_Z = M_{15}^0. \quad (23)$$

However, this unification relation could be modified e.g. due to Φ -insertions, as mentioned above⁷. Similarly, the unification of the Yukawa couplings at the GUT scale,

$$\mathbf{Y}_S = \mathbf{Y}_T = \mathbf{Y}_Z = \mathbf{Y}_{15}^0, \quad (24)$$

could either hold or not. Finally, we stress that in this $SU(5)$ framework the flavour violation is encoded not only in \mathbf{Y}_T (as already elucidated above) but also in \mathbf{Y}_S and \mathbf{Y}_Z . Therefore, non-vanishing barion-flavour violating entries in the mass matrix $\mathbf{m}_{\tilde{d}^c}^2$ of the sdown squarks \tilde{d}^c are induced by radiative corrections. In summary, the three scenarios (A), (B) and (C), put forward in Section 2, can be rephrased as follows:

- (A)- All fragments T, S and Z have the same mass, i.e. eq. (23) holds at M_G . However, the couplings $\mathbf{Y}_S, \mathbf{Y}_Z$ are assumed to be negligible, i.e. eq. (24) does not hold. In this case only the interactions with the triplets T and so the couplings \mathbf{Y}_T drive the lepton-flavour violation in the slepton scalar masses.
- (B)- Both the masses and the Yukawa couplings of the 15 states are unified, i.e. both eqs. (23) and (24) hold. Therefore all the couplings $\mathbf{Y}_S, \mathbf{Y}_T, \mathbf{Y}_Z$ will induce flavour violation in both the slepton \tilde{L} and squark \tilde{d}^c masses.

⁶ Also for the minimal ‘technical’ realization of the doublet-triplet splitting [25] we can give an interpretation of the mass parameter M_5 , analogous to that adopted for the Yukawa couplings, i.e. $M_5(\Phi) = M_5^0 + \lambda_5 \Phi + \dots$.

⁷ Moreover, even if eq. (23) holds at M_G , renormalization effects split the masses at lower energies. However, the relative splitting is not large and we will decouple all the components T, S, Z at the common threshold scale M_T .

- (C)- The triplet mass M_T is much smaller than M_S and M_Z , which are $\mathcal{O}(M_G)$. This could be achieved for instance by tuning the coefficients of the singlet and adjoint components of the 15 $\overline{15}$ ‘mass’, in analogy to what is done for the doublet-triplet splitting for $5_H, \bar{5}_H$.

In the following we shall focus on (A) and (B) and disregard the case (C).

4 \mathbf{Y}_T from neutrino masses and mixing angles

Now, we relate the low-energy parameters with the relevant neutrino Yukawa couplings by adopting a bottom-up criterion. By decoupling the states T, \bar{T} , the $d = 5$ effective operator emerges

$$\frac{\lambda_2}{2M_T} \mathbf{Y}_T^{ij} (L_i H_2) (L_j H_2), \quad (25)$$

where the matrix \mathbf{Y}_T , through the matching of eq. (11), can be connected to \mathbf{Y}_ν which parameterizes the usual $d = 5$ operator (1)⁸.

We recall that the data from solar and atmospheric neutrino experiments concern the neutrino mass eigenvalues m_1, m_2, m_3 and mixing angles. Therefore, in the basis in which the Yukawa matrix \mathbf{Y}_e is diagonal, eqs. (2) and (4) allow us to determine the coupling matrix \mathbf{Y}_ν/M_L at low-energy and then, taking into account the running up to M_T [26], also at the scale M_T .⁹ The mixing matrix \mathbf{U} is parameterised in the standard way:

$$\mathbf{U} = \begin{pmatrix} c_{12}c_{13} & s_{12}c_{13} & s_{13}e^{-i\delta} \\ -s_{12}c_{23} - c_{12}s_{23}s_{13}e^{i\delta} & c_{12}c_{23} - s_{12}s_{23}s_{13}e^{i\delta} & s_{23}c_{13} \\ s_{12}s_{23} - c_{12}c_{23}s_{13}e^{i\delta} & -c_{12}s_{23} - s_{12}c_{23}s_{13}e^{i\delta} & c_{23}c_{13} \end{pmatrix} \quad (26)$$

where s_{ij} and c_{ij} are the cosine and sine respectively of the three mixing angles $\theta_{12}, \theta_{23}, \theta_{13}$ and δ is the CP-violating phase which in the following is neglected for simplicity. As for the phenomenological input, we assume maximal 2-3 mixing, $\theta_{23} = 45^\circ$, as required by the atmospheric neutrino data [6]. We consider hierarchical neutrino mass spectrum, $m_1 \ll m_2 \ll m_3$, such that it reads as:

$$m_1 \approx 0, \quad m_2 = (\Delta m_{\text{sol}}^2)^{1/2}, \quad m_3 = (\Delta m_{\text{atm}}^2)^{1/2}, \quad (27)$$

where we take $\Delta m_{\text{atm}}^2 \sim 3 \times 10^{-3} \text{eV}^2$. As regards the solar neutrino case, the most favoured range for Δm_{sol}^2 is that selected by the large-mixing angle (LMA) solution, $\Delta m_{\text{sol}}^2 \sim 6 \times 10^{-5} \text{eV}^2$ [6]. The corresponding best fit value for the mixing angle is $\theta_{12} \sim 33^\circ$. However, for the sake of discussion in the following we bear in mind also different possibilities, such as the

⁸ The expression given in eq. (25) is the leading contribution to the neutrino mass operator. This arises from the \bar{T} F-term scalar interaction, $\lambda_2 M_T T^* H_2 H_2$. The H_1 F-term scalar interaction, $\mu \lambda_1 H_2^* T H_1$, gives rise to the sub-leading contribution $\lambda_1 (\mu/M_T) (v_2 v_1)/M_T$.

⁹ The radiative corrections from the electroweak scale up to M_T are not important in the case of hierarchical neutrino mass spectrum and amount to an overall common factor [27]. Nevertheless these effects are incorporated in the numerical analysis.

typical values $\Delta m_{\text{sol}}^2 \sim 5 \times 10^{-6} \text{eV}^2$ and $\theta_{12} \sim 4^\circ$ of the small-mixing angle (SMA) solution. Taking also into account the CHOOZ limit, $\sin \theta_{13} < 0.1$ [28], we set $\theta_{13} = 0$ for simplicity and later comment also on the non-zero θ_{13} case. Then at low-energy the symmetric matrix \mathbf{Y}_ν appears as:

$$\mathbf{Y}_\nu = \frac{M_L}{v_2^2} \begin{pmatrix} m_2 s_{12}^2 & \frac{1}{\sqrt{2}} m_2 c_{12} s_{12} & -\frac{1}{\sqrt{2}} m_2 c_{12} s_{12} \\ \frac{1}{2}(m_3 + m_2 c_{12}^2) & \frac{1}{2}(m_3 - m_2 c_{12}^2) & \frac{1}{2}(m_3 + m_2 c_{12}^2) \end{pmatrix}. \quad (28)$$

By considering the phenomenological inputs, we observe that the entries of the 2-3 sector are all comparable and can be of order one (essentially irrespectively of the θ_{12} value) if the scale M_L is close to $M_G \sim 10^{16} \text{GeV}$. The remaining entries are one order of magnitude smaller than those of the 2-3 sector, for θ_{12} in the LMA range, while they are much smaller for θ_{12} in the SMA range. Up to an overall factor due to the renormalization effect, the structure obtained for \mathbf{Y}_ν is finally transferred to \mathbf{Y}_T at the scale M_T according to eq. (11). We stress again that in this T -seesaw scenario the bottom-up approach here adopted is the most general one since the structure of \mathbf{Y}_T is unambiguously fixed by the experimental data themselves. What can be left to our choice is the overall scale M_T/λ_2 . We shall take M_T in the range $10^{11} \div 10^{15} \text{GeV}$ and vary λ_2 in an appropriate range.

5 Lepton-flavour violation in the soft-breaking terms

The general soft SUSY-breaking terms in our model are given as¹⁰:

$$\begin{aligned} -\mathcal{L}_{\text{soft}} = & \tilde{L}^\dagger \mathbf{m}_{\tilde{L}}^2 \tilde{L} + \tilde{e}^c \mathbf{m}_{\tilde{e}^c}^2 \tilde{e}^{c\dagger} + \tilde{d}^c \mathbf{m}_{\tilde{d}^c}^2 \tilde{d}^{c\dagger} + m_{H_1}^2 H_1^\dagger H_1 + m_{H_2}^2 H_2^\dagger H_2 \\ & + (H_1 \tilde{e}^c \mathbf{A}_e \tilde{L} + H_1 \tilde{d}^c \mathbf{A}_d \tilde{Q} + \frac{1}{2} M_a \tilde{\lambda}_a \tilde{\lambda}_a + B\mu H_1 H_2 + \text{h.c.}) \\ & + \left[\frac{1}{\sqrt{2}} (\mathbf{A}_T \tilde{L} T \tilde{L} + \mathbf{A}_S \tilde{d}^c S \tilde{d}^c) + \mathbf{A}_Z \tilde{d}^c Z \tilde{L} + \frac{1}{\sqrt{2}} (A_1 H_1 T H_1 + A_2 H_2 \bar{T} H_2) \right. \\ & \left. + B_T M_T T \bar{T} + B_S M_S S \bar{S} + B_Z M_Z Z \bar{Z} + \text{h.c.} \right] \\ & + m_T^2 T^\dagger T + m_{\bar{T}}^2 \bar{T}^\dagger \bar{T} + m_S^2 S^\dagger S + m_{\bar{S}}^2 \bar{S}^\dagger \bar{S} + m_Z^2 Z^\dagger Z + m_{\bar{Z}}^2 \bar{Z}^\dagger \bar{Z} \end{aligned} \quad (29)$$

where we have shown in the first lines the relevant MSSM terms, according to the standard notation (the soft mass terms for the sleptons, squarks, Higgs bosons, the trilinear terms and the gaugino masses M_a), while in last lines we have collected the new terms involving T, S, Z . In the following we assume at the GUT scale, irrespectively of the scenario (A) or (B)¹¹:

$$\mathbf{m}_{\tilde{L}}^2 = \mathbf{m}_{\tilde{e}^c}^2 = \mathbf{m}_{\tilde{d}^c}^2 = m_0^2 \mathbb{1},$$

¹⁰ For the sake of simplicity, in the following we disregard all what concerns the up-quark sector parameters, such as the scalar masses $\mathbf{m}_{\tilde{Q}}^2$ etc. because they do not enter directly our discussion.

¹¹ These universal boundary conditions are mainly motivated by simplicity and are not assumed for other soft parameters. For instance, we do not declare the soft-breaking mass of the doublet scalar H_2 , as it does not directly enter in our analysis. In this way the μ -parameter in the superpotential is not constrained by

$$\begin{aligned}
m_S^2 &= m_{\bar{S}}^2 = m_T^2 = m_{\bar{T}}^2 = m_Z^2 = m_{\bar{Z}}^2 = m_{H_1}^2 = m_0^2, \\
\mathbf{A}_e &= A_0 \mathbf{Y}_e, \quad \mathbf{A}_d = A_0 \mathbf{Y}_d, \quad A_1 = A_0 \lambda_1, \quad A_2 = A_0 \lambda_2, \\
M_1 &= M_2 = M_3 = M_g,
\end{aligned} \tag{30}$$

where m_0 is the universal scalar mass, A_0 is the universal mass parameter for the trilinear terms and M_g is the common gaugino mass. As for the remaining trilinear couplings, their GUT conditions are in the scenario (A):

$$\mathbf{A}_T = A_0 \mathbf{Y}_T, \quad \mathbf{A}_S = \mathbf{A}_Z = 0, \tag{31}$$

and in the scenario (B)

$$\mathbf{A}_T = \mathbf{A}_S = \mathbf{A}_Z = A_0 \mathbf{Y}_T. \tag{32}$$

The matrix \mathbf{Y}_T which appears in eqs. (31-32) is understood to be evaluated at the GUT scale. Once \mathbf{Y}_T is determined at the scale M_T by the low-energy data as we have seen above, its evolution from M_T up to M_G is given by:

$$\begin{aligned}
16\pi^2 \frac{d\mathbf{Y}_T}{dt} &= \mathbf{Y}_T \left(-\frac{9}{5}g_1^2 - 7g_2^2 + \mathbf{Y}_e^\dagger \mathbf{Y}_e + 6\mathbf{Y}_T^\dagger \mathbf{Y}_T + \text{Tr}(\mathbf{Y}_T \mathbf{Y}_T^\dagger) + 3\mathbf{Y}_Z^\dagger \mathbf{Y}_Z + |\lambda_1|^2 \right) \\
&\quad + (\mathbf{Y}_e^T \mathbf{Y}_e^* + 3\mathbf{Y}_Z^T \mathbf{Y}_Z^*) \mathbf{Y}_T.
\end{aligned} \tag{33}$$

(See also Appendix.) In the scenario (B) the \mathbf{Y}_T RGE is also coupled to those of $\mathbf{Y}_S, \mathbf{Y}_Z$ for which the initial conditions at the scale M_T are determined iteratively under the constraints of eq. (24). Below M_G the universal pattern (30) of $\mathbf{m}_{\bar{L}}^2, \mathbf{m}_{\bar{d}^c}^2$ etc. is spoiled by radiative effects induced by $\mathbf{Y}_T, \mathbf{Y}_S, \mathbf{Y}_Z$. Then we have to evaluate the soft-breaking parameters at low-energy by solving the corresponding RGEs. These have been computed at one-loop and collected in Appendix. In the leptonic sector we need to know the SUSY breaking matrices $\mathbf{m}_{\bar{L}}^2, \mathbf{m}_{\bar{e}^c}^2$ and \mathbf{A}_e to finally compute the LFV decay rates. They all receive flavour blind corrections from the gauge interactions which do not alter the flavour-conserving structure they have at the GUT scale (see eq. (30)). However, they can acquire LFV entries (i.e. off-diagonal entries) if they get radiative corrections from the LFV Yukawa-matrices $\mathbf{Y}_T, \mathbf{Y}_Z$. In the leading-log approximation, and neglecting radiative corrections induced by $\mathbf{Y}_e, \mathbf{Y}_d$, in the picture (A) the LFV entries at low-energy are given by ($i \neq j$):

$$\begin{aligned}
(\mathbf{m}_{\bar{L}}^2)_{ij} &\approx \frac{-1}{8\pi^2} (9m_0^2 + 3A_0^2) (\mathbf{Y}_T^\dagger \mathbf{Y}_T)_{ij} \log \frac{M_G}{M_T}, \\
(\mathbf{m}_{\bar{e}^c}^2)_{ij} &\approx 0, \\
(\mathbf{A}_e)_{ij} &\approx \frac{-9}{16\pi^2} A_0 (\mathbf{Y}_e \mathbf{Y}_T^\dagger \mathbf{Y}_T)_{ij} \log \frac{M_G}{M_T}.
\end{aligned} \tag{34}$$

the electroweak radiative-breaking condition and will be fixed independently. We would like to make clear, however, that the aim of this work is to present the global features of the SUSY T -induced seesaw. Therefore, the choice of these initial conditions, as well as of other parameters such as $\tan\beta$ and μ , which enter in the computations of the decay rates, is only made for illustrative purposes.

and in the picture (B) we find:

$$\begin{aligned}
(\mathbf{m}_{\tilde{L}}^2)_{ij} &\approx \frac{-1}{8\pi^2}(18m_0^2 + 6A_0^2)(\mathbf{Y}_T^\dagger \mathbf{Y}_T)_{ij} \log \frac{M_G}{M_T}, \\
(\mathbf{m}_{\tilde{e}^c}^2)_{ij} &\approx 0, \\
(\mathbf{A}_e)_{ij} &\approx \frac{-9}{8\pi^2}A_0(\mathbf{Y}_e \mathbf{Y}_T^\dagger \mathbf{Y}_T)_{ij} \log \frac{M_G}{M_T},
\end{aligned} \tag{35}$$

and in the squark sector:

$$\begin{aligned}
(\mathbf{m}_{\tilde{d}^c}^2)_{ij} &\approx \frac{-1}{8\pi^2}(18m_0^2 + 6A_0^2)(\mathbf{Y}_T^\dagger \mathbf{Y}_T)_{ij} \log \frac{M_G}{M_T}, \\
(\mathbf{A}_d)_{ij} &\approx \frac{-9}{8\pi^2}A_0(\mathbf{Y}_T^\dagger \mathbf{Y}_T \mathbf{Y}_d)_{ij} \log \frac{M_G}{M_T},
\end{aligned} \tag{36}$$

where we have taken into account the $SU(5)$ -universality for the Yukawa matrices (24). So the mass matrix $\mathbf{m}_{\tilde{e}^c}^2$ remains diagonal and then flavour-conserving, while both $\mathbf{m}_{\tilde{L}}^2$ and \mathbf{A}_e acquire LFV elements. Once the low-energy neutrino observables are fixed, the magnitude of these LFV elements will depend on the matrix $\mathbf{Y}_T^\dagger \mathbf{Y}_T \sim (M_T/\lambda_2 v_2^2)^2 \mathbf{m}_\nu^\dagger \mathbf{m}_\nu$, that is on the triplet mass threshold M_T and on the coupling constant λ_2 . Thus the relative size of LFV in the 2-3 sector and 1-2 sector can be approximately predicted in terms of only the low-energy observables, as we anticipated in eq. (16). Such a ratio can be rewritten more explicitly:

$$\frac{(\mathbf{m}_{\tilde{L}}^2)_{\tau\mu}}{(\mathbf{m}_{\tilde{L}}^2)_{\mu e}} \approx \left(\frac{m_3}{m_2}\right)^2 \frac{\sin 2\theta_{23}}{\sin 2\theta_{12} \cos \theta_{23}} \sim 80, \tag{37}$$

where for the estimate we have taken for θ_{12} and m_2 the values selected by the LMA solution. For the case of SMA solution that ratio increases to $10^3 - 10^4$. These results clearly hold in both scenarios (A) and (B). Therefore, this estimate can directly be translated into a prediction for the ratio of the decay rate of $\tau \rightarrow \mu\gamma$ and $\mu \rightarrow e\gamma$ as we shall show in the next Section. We also recall that since $\theta_{23} \sim 45^\circ$, the first generation is mixed with a state which is an equal (and indistinguishable) mixture of the flavour states ν_μ, ν_τ . It is not surprising therefore that the ratio $(\mathbf{m}_{\tilde{L}}^2)_{\tau e}/(\mathbf{m}_{\tilde{L}}^2)_{\mu e}$ be of order one:

$$\frac{(\mathbf{m}_{\tilde{L}}^2)_{\tau e}}{(\mathbf{m}_{\tilde{L}}^2)_{\mu e}} \approx \tan \theta_{23} \sim 1. \tag{38}$$

Notice also that the size of the lepton-flavour violating entries $(\mathbf{m}_{\tilde{L}}^2)_{ij}$ is about a factor 2 larger in the scenario (B) due to the extra contribution driven by the Yukawa couplings $\mathbf{Y}_{Z,S}$. This implies that the related decay-rates are further enhanced by a factor 4 in the scenario (B). Moreover, in the scenario (B), we have similar predictions for the sdown sector, namely:

$$\frac{(\mathbf{m}_{\tilde{d}^c}^2)_{bs}}{(\mathbf{m}_{\tilde{d}^c}^2)_{sd}} \approx \left(\frac{m_3}{m_2}\right)^2 \frac{\sin 2\theta_{23}}{\sin 2\theta_{12} \cos \theta_{23}} \sim 80, \quad \frac{(\mathbf{m}_{\tilde{d}^c}^2)_{bd}}{(\mathbf{m}_{\tilde{d}^c}^2)_{sd}} \approx \tan \theta_{23} \sim 1, \tag{39}$$

which show that the relative flavour-violation in the lepton and quark sector should be comparable in magnitude.

Finally, we would like to comment also upon the case in which the 1-3 mixing is restored in the lepton mixing matrix. So for discussion we consider the present upper bound on θ_{13} [28] and take $\sin \theta_{13} = 0.1$. This leads to an enhancement of the LFV entries $(\mathbf{m}_L^2)_{\mu e}$ and $(\mathbf{m}_L^2)_{\tau e}$ driven by the largest mass m_3 , with respect to the $\theta_{13} = 0$, namely

$$\begin{aligned}\frac{(\mathbf{m}_L^2)_{\mu e}|_{\theta_{13} \neq 0}}{(\mathbf{m}_L^2)_{\mu e}|_{\theta_{13} = 0}} &\approx 1 + \left(\frac{m_3}{m_2}\right)^2 \frac{\sin \theta_{13}}{\sin \theta_{12} \cos \theta_{12}} \sim 10, \\ \frac{(\mathbf{m}_L^2)_{\tau e}|_{\theta_{13} \neq 0}}{(\mathbf{m}_L^2)_{\tau e}|_{\theta_{13} = 0}} &\approx 1 - \left(\frac{m_3}{m_2}\right)^2 \frac{\sin \theta_{13}}{\sin \theta_{12} \cos \theta_{12}} \sim -10.\end{aligned}\quad (40)$$

Therefore, since the entry $(\mathbf{m}_L^2)_{\tau \mu}$ is not modified, the ratio of eq. (37) becomes ~ 7 , while that in eq. (38) remains the same. By considering the values for m_2 and θ_{12} of the SMA solution, we find for $\sin \theta_{13} = 0.1$ a much stronger relative enhancement,

$$\begin{aligned}\frac{(\mathbf{m}_L^2)_{\mu e}|_{\theta_{13} \neq 0}}{(\mathbf{m}_L^2)_{\mu e}|_{\theta_{13} = 0}} &\approx 10^3, \\ \frac{(\mathbf{m}_L^2)_{\tau e}|_{\theta_{13} \neq 0}}{(\mathbf{m}_L^2)_{\tau e}|_{\theta_{13} = 0}} &\approx -10^3.\end{aligned}\quad (41)$$

Analogous results are obtained for the entries $(\mathbf{m}_{\tilde{d}c}^2)_{ij}$.

6 The $\ell_i \rightarrow \ell_j \gamma$ decay rates

Let us briefly recall here some points related to the computation of the $\ell_i \rightarrow \ell_j \gamma$ decay rate. The effective operator responsible for such a decay can be parameterised as

$$\mathcal{L}_{\text{eff}} = ig_e m_i (C_L^{ij} \bar{\ell}_j \bar{\sigma}^{\mu\nu} \bar{\ell}_i^c + C_R^{ij} \bar{\ell}_j^c \sigma^{\mu\nu} \ell_i) F_{\mu\nu}, \quad (42)$$

where g_e is the electromagnetic coupling and we use two-component spinor notation. This leads to the branching ratio

$$BR(\ell_i \rightarrow \ell_j \gamma) = \frac{48\pi^3 \alpha_{\text{em}}}{G_F^2} (|C_L^{ij}|^2 + |C_R^{ij}|^2) BR(\ell_i \rightarrow \ell_j \nu_i \bar{\nu}_j), \quad (43)$$

where in the specific cases the lepton-flavour conserving branching ratio are $BR(\mu \rightarrow e \nu_\mu \bar{\nu}_e) \approx 1$, $BR(\tau \rightarrow \mu \nu_\tau \bar{\nu}_\mu) \approx 17\%$ and $BR(\tau \rightarrow e \nu_\tau \bar{\nu}_e) \approx 18\%$. For the numerical analysis we have taken into account all contributions involving one-loop slepton-chargino and slepton-neutralino exchange, by using the complete formulas given for example in ref. [16]. Analogously to the case of the MSSM with singlets N [16], also in this scenario the main contributions come from $\tan \beta$ -enhanced diagrams with chargino exchange. In the mass-insertion approximation, we recall that the parameter dependence of C_L^{ij} (the dominant coefficient) is

$$C_L^{ij} \sim \frac{g^2}{16\pi^2} \frac{(\mathbf{m}_L^2)_{ij}}{\tilde{m}^4} \tan \beta, \quad (44)$$

where \tilde{m} is an average soft mass.

The main feature of our picture is the possibility to relate in a *model-independent* way the LFV of different sectors, as eqs. (16) and (17) demonstrate. Therefore, if we take the corresponding ratio of the BRs and take into account the estimate in (37), we find:

$$\frac{BR(\tau \rightarrow \mu\gamma)}{BR(\mu \rightarrow e\gamma)} \approx \left(\frac{(\mathbf{m}_L^2)_{\tau\mu}}{(\mathbf{m}_L^2)_{\mu e}} \right)^2 \frac{BR(\tau \rightarrow \mu\nu_\tau\bar{\nu}_\mu)}{BR(\mu \rightarrow e\nu_\mu\bar{\nu}_e)} \sim 10^3. \quad (45)$$

For the case of SMA solution, this would become much larger, i.e. $\sim 10^7$. Analogously we can predict

$$\frac{BR(\tau \rightarrow e\gamma)}{BR(\mu \rightarrow e\gamma)} \approx \left(\frac{(\mathbf{m}_L^2)_{\tau e}}{(\mathbf{m}_L^2)_{\mu e}} \right)^2 \frac{BR(\tau \rightarrow e\nu_\tau\bar{\nu}_e)}{BR(\mu \rightarrow e\nu_\mu\bar{\nu}_e)} \sim 10^{-1}. \quad (46)$$

Let us now discuss the results obtained by a more detailed numerical study with exact solutions of the RGEs and exact diagonalization of matrices involved in the computation of the branching ratios. First in Fig. 2 we present the behaviour of the LFV parameters $\delta_{ij}^{\tilde{L}}$ and $\delta_{ij}^{\tilde{d}^c}$ defined as

$$\delta_{ij}^{\tilde{L}} = \frac{|(\mathbf{m}_L^2)_{ij}|}{m_{\tilde{L}}^2}, \quad \delta_{ij}^{\tilde{d}^c} = \frac{|(\mathbf{m}_{\tilde{d}^c}^2)_{ij}|}{m_{\tilde{d}^c}^2}, \quad (47)$$

($m_{\tilde{L}}^2, m_{\tilde{d}^c}^2$ are the average \tilde{L} and \tilde{d}^c squared masses) as a function of the coupling λ_2 in both scenarios (A) and (B), for two values of M_T , i.e. $M_T = 10^{11}$ GeV (upper left panel) and $M_T = 10^{14}$ GeV (upper right panel) and for representative values of other parameters. For each scenario the upper and lower curve refers to $\delta_{\tau\mu}^{\tilde{L}}$ and $\delta_{\mu e}^{\tilde{L}}$ (or $\delta_{\tau e}^{\tilde{L}}$, cfr. eq. (38)), respectively, and similarly for $\delta_{bs}^{\tilde{d}^c}$ and $\delta_{sd}^{\tilde{d}^c}$, in the scenario (B). Due to the quadratic dependence in the RGEs on the LFV Yukawa matrices $\mathbf{Y}_T, \mathbf{Y}_S, \mathbf{Y}_Z$, the δ parameters scale as $(\lambda_2)^{-2}$. We notice that the size of LFV in the 2-3 and 1-2 sectors maintains a constant ratio, $\sim 10^2$, independently of the scale M_T (cfr. the estimate in eq. (37)). In correspondence of each value of the scale M_T , there is a minimum value for λ_2 , below which the RGE solutions blow up¹², which is approximately $\lambda_2^{\min} \sim 3 \times 10^{-4} (M_T/10^{11} \text{ GeV})$. We can notice that in the scenario (B) $\delta_{ij}^{\tilde{L}}$ gets larger than in case (A) by about a factor 2. Moreover, $\delta_{ij}^{\tilde{d}^c}$ are about a factor 2 smaller than $\delta_{ij}^{\tilde{L}}$. This is due to the fact that in the evolution to low-energy the squark mass gets heavier than the slepton mass, because of the gluino-driving. This different increase is reflected mostly in the average scalar masses (which are determined at the SUSY scale) and to a less extent in the off-diagonal entries $(\mathbf{m}_L^2)_{ij}, (\mathbf{m}_{\tilde{d}^c}^2)_{ij}$ (which instead are determined at the intermediate scale M_T). The partial compensation of these effects explains why, for $M_T = 10^{11}$ GeV, for instance, the ratio $\delta^{\tilde{L}}/\delta^{\tilde{d}^c}$ is smaller than 4, even though $m_{\tilde{L}} \sim 300$ GeV and $m_{\tilde{d}^c} \sim 600$ GeV.

In the same figure we also show the behaviour of the branching ratios (lower panels) for $\tan\beta = 3$, as a representative case. For each decay the lower and upper curve refers to the scenario (A) and (B), respectively. It is striking to notice that the constant-ratio rule

¹² One has also to check that λ_2 is not too large at M_T so that it remains perturbative up to M_G (cfr. the λ_2 -RGE in eq. (51) in Appendix).

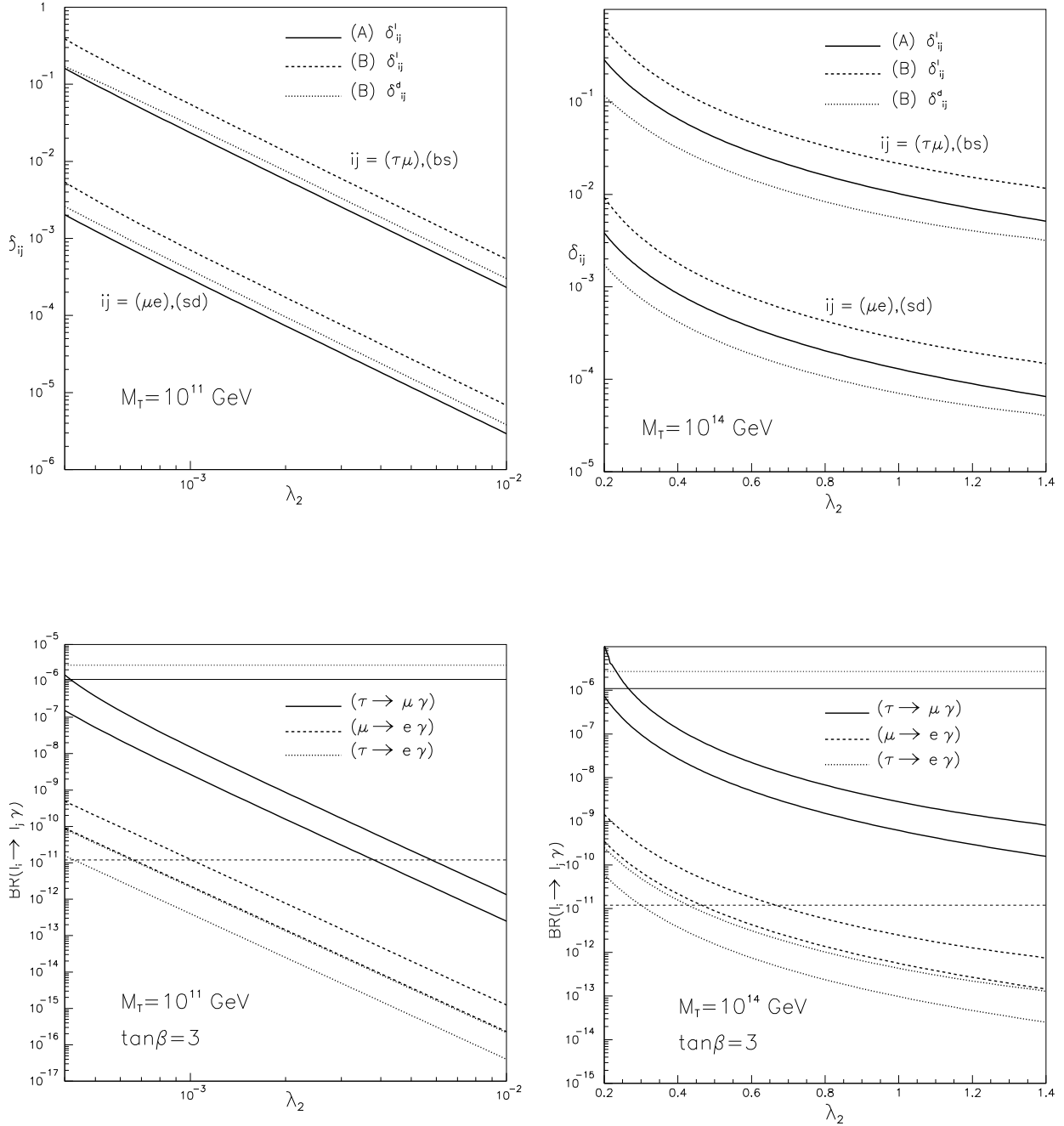


Figure 2: In the upper panels we show the flavour-violation parameters $\delta^{\tilde{L}}$ and $\delta^{\tilde{d}c}$ as a function of the coupling constant λ_2 (at M_T) for $M_T = 10^{11}$ GeV (left) and $M_T = 10^{14}$ GeV (right) in both scenarios (A) and (B). As for the neutrino parameters, we have taken $\theta_{23} = 45^\circ, \theta_{12} = 33^\circ, \theta_{13} = 0$ and $m_1 = 0, m_2 = 7 \times 10^{-3}$ eV, $m_3 = 5 \times 10^{-2}$ eV. In correspondence of each scenario, the upper lines refer to $\delta_{\tau\mu}^{\tilde{L}}$ and $\delta_{bs}^{\tilde{d}c}$ and the lower ones to $\delta_{\mu e}^{\tilde{L}}$ and $\delta_{sd}^{\tilde{d}c}$ (the $\delta^{\tilde{d}c}$ are non-zero only in the case (B)). We recall that $\delta_{\tau e}^{\tilde{L}} = \delta_{\mu e}^{\tilde{L}}$ as well as $\delta_{bd}^{\tilde{d}c} = \delta_{sd}^{\tilde{d}c}$. In the lower panels we show the resulting branching-ratios for the decays $\tau \rightarrow \mu \gamma, \mu \rightarrow e \gamma$ and $\tau \rightarrow e \gamma$. The horizontal lines denote the experimental upper bounds of such BRs. For each BR the lower and upper curve is obtained in the scenario (A) and (B), respectively. In all panels, we have fixed $A_0 = m_0 = 200$ GeV at M_G ; the corresponding average slepton mass at low energy is $m_{\tilde{L}} \sim 300$ GeV (250 GeV) for $M_T = 10^{11}$ GeV (10^{14} GeV). Finally, the parameters fixed at low energies are $\tan \beta = 3$, $\mu = 300$ GeV and $M_2 = 180$ GeV; the latter corresponds to $M_g = 490$ GeV (290 GeV) at M_G for $M_T = 10^{11}$ GeV (10^{14} GeV). We have also set $\lambda_1 = \lambda_2$ at M_T .

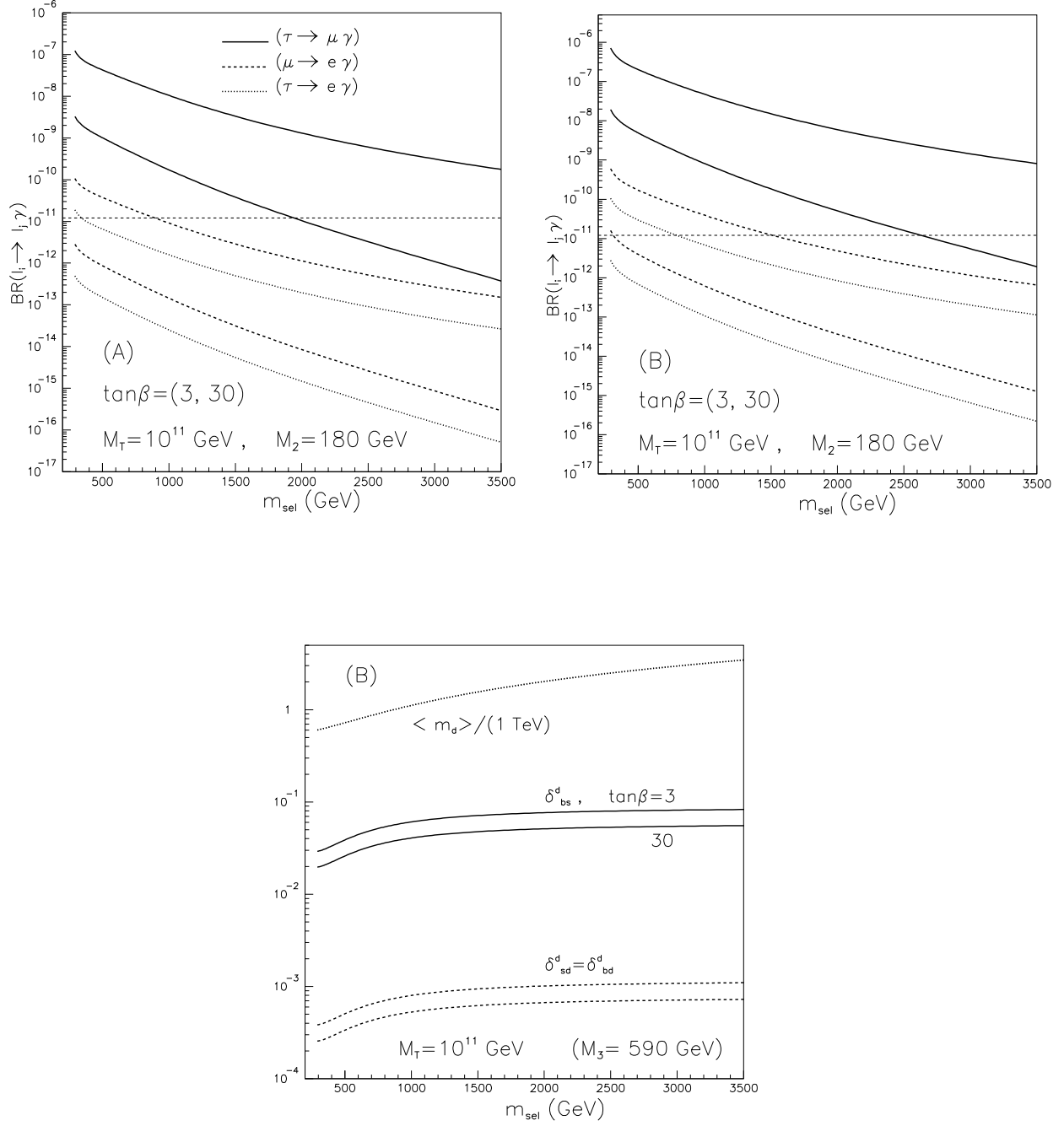


Figure 3: In the upper panels we display the behaviour of the $\ell_i \rightarrow \ell_j \gamma$ BRs as a function of the ‘left-handed’ selectron mass in both scenarios (A) (left panel) and (B) (right panel) for $M_T = 10^{11}$ GeV and $\lambda_2 = 10^{-3}$ (at M_T). For each BR the lower and upper line refers to the case with $\tan \beta = 3$ and 30, respectively. The horizontal dashed-line marks the $BR(\mu \rightarrow e \gamma)$ experimental bound. The gaugino mass and μ have been taken as in Fig. 2. In the lower panel we show the corresponding parameters δ_{ij}^d as emerge in the scenario (B), as a function of the selectron mass (solid and dashed lines). The dotted lines denotes the average $m_{\tilde{d}^c}$ mass. The value of the gluino mass M_3 as obtained at low energy is also indicated.

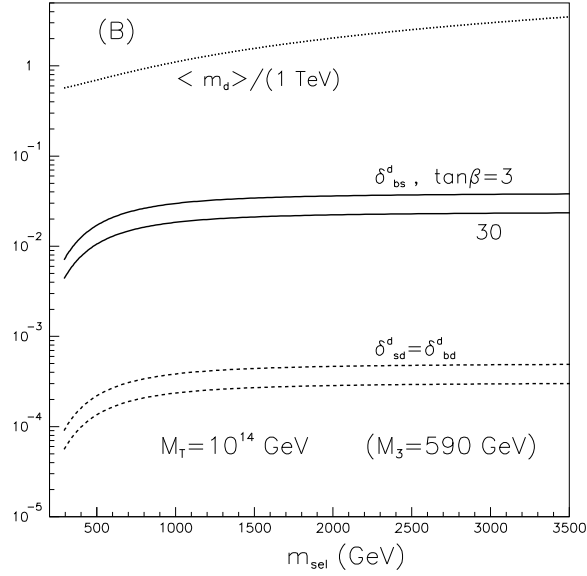
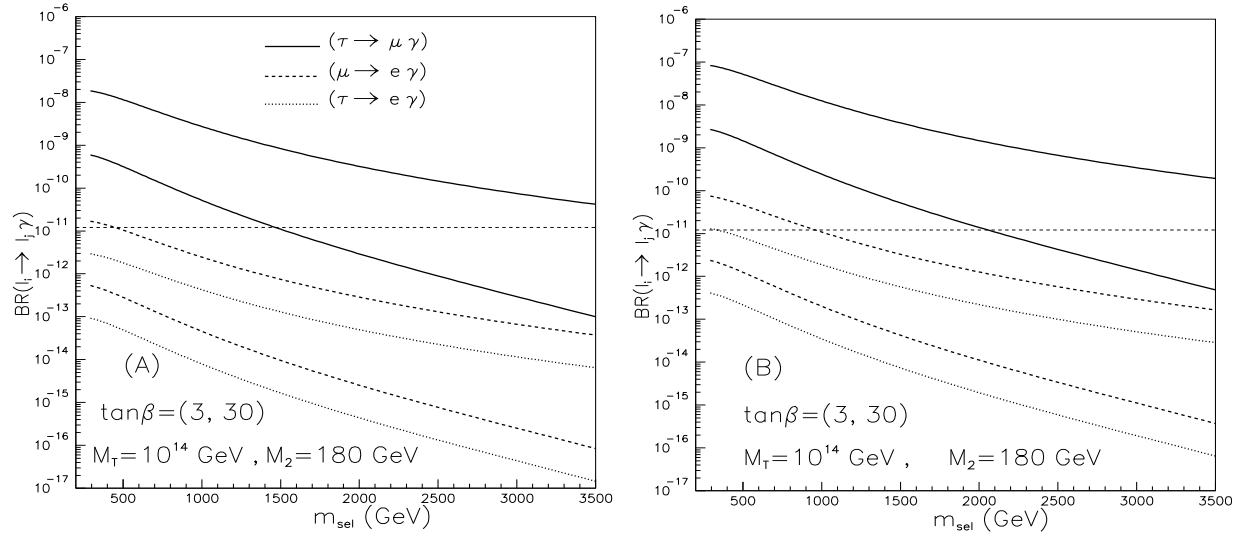


Figure 4: The same as in Fig. 3 for $M_T = 10^{14}$ GeV and $\lambda_2 = 1$.

displayed in eqs. (45- 46) between the BR of the decays $\tau \rightarrow \mu\gamma$ or $\tau \rightarrow e\gamma$ with that of $\mu \rightarrow e\gamma$ is preserved in each case (A) and (B) as well as for any value of M_T , irrespectively of the value of λ_2 . Moreover, in the scenario (B) with all the Yukawa couplings $\mathbf{Y}_{T,S,Z}$ at work these rates are larger since the LFV in the slepton masses is enhanced, as seen in the upper panels. The present bound on the $BR(\mu \rightarrow e\gamma)$ (shown by dashed horizontal line) constrains λ_2 to be larger than $\sim 7 \times 10^{-4}$ and ~ 0.46 for $M_T = 10^{11}$ GeV and 10^{14} GeV, respectively in the case (A). In the picture (B) these bounds get a bit more stringent, $\lambda_2 \gtrsim 2 \times 10^{-3}$ and $\lambda_2 \gtrsim 0.65$ for $M_T = 10^{11}$ GeV and 10^{14} GeV, respectively. The T -induced seesaw strict predictions for the ratio of the BR s tell us that, in view of the future experimental sensitivity, both decays $\tau \rightarrow \mu\gamma$ and $\mu \rightarrow e\gamma$ could be observed if the latter has at least a branching ratio of order 10^{-12} . For $BR(\mu \rightarrow e\gamma) < 10^{-12}$, we have that $BR(\tau \rightarrow \mu\gamma) < 10^{-9}$, below the expected sensitivity. On the other hand, if we depart from the limit $\theta_{13} = 0$ and allow θ_{13} as large as 0.1, we would get $BR(\tau \rightarrow \mu\gamma) \sim 10 \cdot BR(\mu \rightarrow e\gamma)$. As for $BR(\tau \rightarrow e\gamma)$ it is always predicted to be one order of magnitude smaller than $BR(\mu \rightarrow e\gamma)$.

In Fig. 3 we show $BR(\mu \rightarrow e\gamma)$, $BR(\tau \rightarrow \mu\gamma)$ and $BR(\tau \rightarrow e\gamma)$ as a function of the left-handed selectron mass at low-energy with $M_T = 10^{11}$ GeV and $\lambda_2 = 10^{-3}$ for both scenarios (A) (upper left panel) and (B) (upper right panel). For each BR , the upper and lower curves correspond to $\tan \beta = 30$ and 3, respectively. In the scenario (A) for $\tan \beta = 3$ there are no constraints on $m_{\tilde{e}}$ from the $BR(\mu \rightarrow e\gamma)$ bound, while for $\tan \beta = 30$ we have $m_{\tilde{e}} \gtrsim 900$ GeV. More stringent lower bounds on $m_{\tilde{e}}$ can be deduced in the scenario (B). Therefore in the allowed range for $m_{\tilde{e}}$, we have $BR(\tau \rightarrow \mu\gamma) \lesssim 2 \times 10^{-8}$ and $BR(\tau \rightarrow e\gamma) \lesssim 2 \times 10^{-12}$. Again notice that the constant-ratio rule for the BR s is maintained also in this case where $m_{\tilde{e}}$ is varied, confirming the fact that this rule depends only on the low-energy neutrino parameters and not on the details of the model, such as the soft-breaking parameters or M_T . In the lower panel, we show the behaviour of $\delta^{\tilde{d}^c}$ and the average squark mass $m_{\tilde{d}^c}$ versus $m_{\tilde{e}}$. The fact that $\delta^{\tilde{d}^c}$ are about a factor 1.5 larger for $\tan \beta = 3$ as compared to the case with $\tan \beta = 30$ is due to the combined increase for lower values of $\tan \beta$ of both \mathbf{Y}_ν (see eq. 12)) and the top Yukawa coupling, $Y_t \sim m_t/(v \sin \beta)$, which influences the running of \mathbf{Y}_ν from low-energy up to M_T (see eq. (56) in Appendix). We recall that the whole increase of \mathbf{Y}_ν implies an increase of \mathbf{Y}_T as well of \mathbf{Y}_Z and \mathbf{Y}_S through the relation (24). Then the quantities $\mathbf{Y}_Z \mathbf{Y}_Z^\dagger$ and $\mathbf{Y}_S \mathbf{Y}_S^\dagger$ (scaling as $1/\sin^4 \beta$) trigger the flavour-violation in the matrix $\mathbf{m}_{\tilde{d}^c}$. The information on $\delta^{\tilde{d}^c}$ and $m_{\tilde{d}^c}$ could be useful for the comparison with the present bounds on the flavour-violation parameters $\delta^{\tilde{d}^c}$ extracted from the meson mixing measurements [29]. To this purpose we need to know also that the gluino mass at low-energy is $M_3 \sim 600$ GeV for $M_T = 10^{11}$ GeV. For example, for $\tan \beta = 3$ and $m_{\tilde{e}} > 300$ GeV, we have $m_{\tilde{d}^c} \sim 600$ GeV and $\delta_{sd}^{\tilde{d}^c}$ (or $\delta_{bd}^{\tilde{d}^c}$) $\approx 4 \times 10^{-4}$ which is below the limits from the $K^0 - \bar{K}^0$ (or $B_d - \bar{B}_d$) mixing parameter.

In Fig. 4 the same analysis has been performed for $M_T = 10^{14}$ GeV and we have chosen $\lambda_2 = 1$, in such a way that the ratio M_T/λ_2 is the same as in the previous example. In this way, the size of the matrix \mathbf{Y}_T is the same at the scale M_T . All other parameters, such as M_2 at low energy, are the same as in Fig. 3. Upon comparing with the previous case with lower M_T , we observe that for larger M_T the BRs are smaller by a factor 5 which is due to the smaller energy interval of the running, namely $[\log(M_G/10^{11} \text{ GeV})/\log(M_G/10^{14} \text{ GeV})]^2 \approx$

5. For the same reason, for $M_T = 10^{14}$ GeV the parameters $\delta^{\tilde{d}^c}$ are smaller by a factor 2 or so.

7 Conclusions

The neutrino experimental observations pointing to sizeable lepton mixing have been encouraging to further investigate the implications of lepton-flavour violation in extensions of the Standard Model. This work may be placed among these attempts. In particular, we have considered the SUSY seesaw mechanism obtained through the exchange of heavy $SU(2)$ triplets. On comparing with the more popular seesaw scenario with the exchange of heavy singlets, our scenario is more predictive since the source of LFV at high energy, i.e. the Yukawa matrix \mathbf{Y}_T , can be directly connected to the low-energy observables, encoded in the coupling matrix \mathbf{Y}_ν . The Yukawa \mathbf{Y}_T induces radiative corrections in the mass matrix of the sleptons \tilde{L} and as a result, even in the case of universal scalar masses at the GUT scale, LFV off-diagonal entries are generated. Therefore the flavour structure of the slepton mass matrix can be determined solely in terms of the low-energy neutrino parameters, i.e. the neutrino masses and mixing angles. The most remarkable feature of this scenario is that there is a rigid entanglement of the flavour-violation among different generations, as displayed in eqs. (37-38), which does not depend on other details of the theoretical framework. This implies in particular that the ratio of the branching ratios of the decay $\tau \rightarrow \mu\gamma$ (or $\tau \rightarrow e\gamma$) and $\mu \rightarrow e\gamma$ can be predicted and turns out to be $\sim 10^3$ (or 10^{-1}). We have first derived these estimates by only taking into account the neutrino parameters (45-46) and have confirmed them by more detailed numerical computations, as shown in Figs. 2, 3 and 4. Furthermore we have embedded this picture in a ‘minimal’ $SU(5)$ scenario in which the triplet states T fill the 15-representation together with other coloured partners S, Z . In such a case flavour violation is also induced by radiative corrections on the mass matrix of the d^c -squarks. By imposing the GUT scale $SU(5)$ -universality relation among the Yukawa couplings of those states to the matter multiplets, we find that the size of flavour violation in the lepton and quark sectors is comparable. This implies that, similarly to what happens in the lepton sector, the amount of flavour-violation between different quark sectors is strongly correlated. For example, one could predict the supersymmetric contribution to $B_s - \bar{B}_s$ mixing in terms of that to $K^0 - \bar{K}^0$ mixing. It would be interesting to further explore this point and other implications of the SUSY T -induced seesaw.

Acknowledgments This work was partially supported by the European Union under the contracts HPRN-CT-2000-00148 (Across the Energy Frontier) and HPRN-CT-2000-00149 (Collider Physics).

Appendix

In this appendix we first present the parametrization used for the chargino and neutralino

mass matrix since this determines the relative sign between the Yukawa and gauge terms¹³ in the renormalization group equations of the trilinear soft-breaking terms (see below (55)). Then we have determined the renormalization group equations in the MSSM with the $15 + \overline{15}$ representation of $SU(5)$ at one-loop, which are therefore valid in the energy range between M_G and the triplet mass scale M_T .

The chargino mass matrix term is given by:

$$-\mathcal{L}_{\text{ch}} = \begin{pmatrix} \tilde{W}^+ \\ \tilde{H}_2^+ \end{pmatrix}^T \begin{pmatrix} M_2 & gv_2 \\ gv_1 & \mu \end{pmatrix} \begin{pmatrix} \tilde{W}^- \\ \tilde{H}_2^- \end{pmatrix} + \text{h.c.}, \quad (48)$$

and that regarding the neutralino mass sector is:

$$-\mathcal{L}_n = \frac{1}{2} \begin{pmatrix} \tilde{B} \\ \tilde{W}^0 \\ \tilde{H}_1^0 \\ \tilde{H}_2^0 \end{pmatrix}^T \begin{pmatrix} M_1 & 0 & -\frac{1}{\sqrt{2}}g'v_1 & \frac{1}{\sqrt{2}}g'v_2 \\ 0 & M_2 & \frac{1}{\sqrt{2}}gv_1 & -\frac{1}{\sqrt{2}}gv_2 \\ -\frac{1}{\sqrt{2}}g'v_1 & \frac{1}{\sqrt{2}}gv_1 & 0 & -\mu \\ \frac{1}{\sqrt{2}}g'v_2 & -\frac{1}{\sqrt{2}}gv_2 & -\mu & 0 \end{pmatrix} \begin{pmatrix} \tilde{B} \\ \tilde{W}^0 \\ \tilde{H}_1^0 \\ \tilde{H}_2^0 \end{pmatrix} + \text{h.c.} \quad (49)$$

The renormalization group equations for the gaugino masses M_a , ($a = 1, 2, 3$) are:

$$16\pi^2 \frac{dM_a}{dt} = 2g_a^2 B_a M_a, \quad (50)$$

where the coefficients B_a are given in eq. (19). The RGEs for the Yukawa couplings are:

$$\begin{aligned} 16\pi^2 \frac{d\mathbf{Y}_T}{dt} &= \mathbf{Y}_T \left[-\frac{9}{5}g_1^2 - 7g_2^2 + \mathbf{Y}_e^\dagger \mathbf{Y}_e + 6\mathbf{Y}_T^\dagger \mathbf{Y}_T + \text{Tr}(\mathbf{Y}_T^\dagger \mathbf{Y}_T) + \mathbf{Y}_Z^\dagger \mathbf{Y}_Z + |\lambda_1|^2 \right] \\ &\quad + (\mathbf{Y}_e^T \mathbf{Y}_e^* + \mathbf{Y}_Z^T \mathbf{Y}_Z^*) \mathbf{Y}_T, \\ 16\pi^2 \frac{d\mathbf{Y}_S}{dt} &= \mathbf{Y}_S \left[-\frac{4}{5}g_1^2 - 12g_3^2 + 2\mathbf{Y}_d^* \mathbf{Y}_d^T + 8\mathbf{Y}_S^\dagger \mathbf{Y}_S + \text{Tr}(\mathbf{Y}_S^\dagger \mathbf{Y}_S) + 2\mathbf{Y}_Z^* \mathbf{Y}_Z^T \right] \\ &\quad + 2(\mathbf{Y}_d \mathbf{Y}_d^\dagger + \mathbf{Y}_Z \mathbf{Y}_Z^\dagger) \mathbf{Y}_S, \\ 16\pi^2 \frac{d\mathbf{Y}_Z}{dt} &= \mathbf{Y}_Z \left[-\frac{7}{15}g_1^2 - 3g_3^2 - \frac{16}{3}g_3^2 + \mathbf{Y}_e^\dagger \mathbf{Y}_e + 5\mathbf{Y}_Z^\dagger \mathbf{Y}_Z + \text{Tr}(\mathbf{Y}_Z^\dagger \mathbf{Y}_Z) + 3\mathbf{Y}_T^\dagger \mathbf{Y}_T \right] \\ &\quad + 2(\mathbf{Y}_d \mathbf{Y}_d^\dagger + 2\mathbf{Y}_S \mathbf{Y}_S^\dagger) \mathbf{Y}_Z, \\ 16\pi^2 \frac{d\mathbf{Y}_e}{dt} &= \mathbf{Y}_e \left[-\frac{27}{15}g_1^2 - 3g_2^2 + 3(\mathbf{Y}_e^\dagger \mathbf{Y}_e + \mathbf{Y}_T^\dagger \mathbf{Y}_T + \mathbf{Y}_Z^\dagger \mathbf{Y}_Z + |\lambda_1|^2) + \text{Tr}(\mathbf{Y}_e^\dagger \mathbf{Y}_e + 3\mathbf{Y}_d^\dagger \mathbf{Y}_d) \right], \\ 16\pi^2 \frac{d\mathbf{Y}_d}{dt} &= \mathbf{Y}_d \left[-\frac{7}{15}g_1^2 - 3g_2^2 - \frac{16}{3}g_3^2 + 3(\mathbf{Y}_d^\dagger \mathbf{Y}_d + |\lambda_1|^2) + \mathbf{Y}_u^\dagger \mathbf{Y}_u \right. \\ &\quad \left. + \text{Tr}(\mathbf{Y}_e^\dagger \mathbf{Y}_e + 3\mathbf{Y}_d^\dagger \mathbf{Y}_d) \right] + 2(\mathbf{Y}_Z \mathbf{Y}_Z^\dagger + 2\mathbf{Y}_S \mathbf{Y}_S^\dagger) \mathbf{Y}_d, \end{aligned}$$

¹³ We have indeed found some discrepancy in the literature. Our results, for example, are in agreement with the RGEs of [30]. In the latter work there is consistency between the sign of the gaugino mass terms and the RGEs of the trilinear terms provided a (missed) minus sign is accounted in front of the gaugino mass in the matrix of eq. (2.7) (or, equivalently, provided the i factor in the off-diagonal blocks is removed).

$$\begin{aligned}
16\pi^2 \frac{d\mathbf{Y}_u}{dt} &= \mathbf{Y}_u \left[-\frac{13}{15}g_1^2 - 3g_2^2 - \frac{16}{3}g_3^2 + 3\mathbf{Y}_u^\dagger \mathbf{Y}_u + \mathbf{Y}_d^\dagger \mathbf{Y}_d + 3|\lambda_2|^2 + 3\text{Tr}(\mathbf{Y}_u^\dagger \mathbf{Y}_u) \right], \\
16\pi^2 \frac{d\lambda_1}{dt} &= \lambda_1 \left[7\lambda_1^2 + \text{Tr}(\mathbf{Y}_T \mathbf{Y}_T^\dagger + 2\mathbf{Y}_e \mathbf{Y}_e^\dagger + 6\mathbf{Y}_d \mathbf{Y}_d^\dagger) - \frac{9}{5}g_1^2 - 7g_2^2 \right], \\
16\pi^2 \frac{d\lambda_2}{dt} &= \lambda_2 \left[7\lambda_2^2 + 6\text{Tr}(\mathbf{Y}_u \mathbf{Y}_u^\dagger) - \frac{9}{5}g_1^2 - 7g_2^2 \right], \tag{51}
\end{aligned}$$

where \mathbf{Y}_d and \mathbf{Y}_u are the Yukawa coupling matrix of the down and up quarks, respectively. Regarding the mass parameters of the superpotential, the RGEs are:

$$\begin{aligned}
16\pi^2 \frac{d\mu}{dt} &= \mu \left[3\text{Tr}(\mathbf{Y}_u^\dagger \mathbf{Y}_u + \mathbf{Y}_d^\dagger \mathbf{Y}_d) + \text{Tr}(\mathbf{Y}_e^\dagger \mathbf{Y}_e) + 3(|\lambda_1|^2 + |\lambda_2|^2) - \frac{3}{5}g_1^2 - 3g_2^2 \right], \\
16\pi^2 \frac{dM_T}{dt} &= M_T \left[\text{Tr}(\mathbf{Y}_T^\dagger \mathbf{Y}_T) + |\lambda_1|^2 + |\lambda_2|^2 - \frac{3}{5}g_1^2 - 8g_2^2 \right], \\
16\pi^2 \frac{dM_S}{dt} &= M_S \left[\text{Tr}(\mathbf{Y}_S^\dagger \mathbf{Y}_S) - \frac{16}{15}g_1^2 - \frac{40}{3}g_3^2 \right], \\
16\pi^2 \frac{dM_Z}{dt} &= M_Z \left[\text{Tr}(\mathbf{Y}_Z^\dagger \mathbf{Y}_Z) - \frac{1}{15}g_1^2 - 3g_2^2 - \frac{16}{3}g_3^2 \right]. \tag{52}
\end{aligned}$$

The RGEs for the sfermion mass matrices are:

$$\begin{aligned}
16\pi^2 \frac{d\mathbf{m}_{\tilde{L}}^2}{dt} &= \mathbf{m}_{\tilde{L}}^2 (\mathbf{Y}_e^\dagger \mathbf{Y}_e + 3\mathbf{Y}_T^\dagger \mathbf{Y}_T + 3\mathbf{Y}_Z^\dagger \mathbf{Y}_Z) + (\mathbf{Y}_e^\dagger \mathbf{Y}_e + 3\mathbf{Y}_T^\dagger \mathbf{Y}_T + 3\mathbf{Y}_Z^\dagger \mathbf{Y}_Z) \mathbf{m}_{\tilde{L}}^2 \\
&\quad + 2 \left(\mathbf{Y}_e^\dagger m_{H_1}^2 \mathbf{Y}_e + \mathbf{Y}_e^\dagger m_{\tilde{e}^c}^2 \mathbf{Y}_e + 3\mathbf{Y}_T^\dagger \mathbf{m}_{\tilde{L}}^2 \mathbf{Y}_T + 3\mathbf{Y}_Z^\dagger \mathbf{m}_{\tilde{d}^c}^2 \mathbf{Y}_Z + 3\mathbf{Y}_T^\dagger m_T^2 \mathbf{Y}_T \right. \\
&\quad \left. + 3\mathbf{Y}_Z^\dagger m_Z^2 \mathbf{Y}_Z \right) + 2(\mathbf{A}_e^\dagger \mathbf{A}_e + 3\mathbf{A}_T^\dagger \mathbf{A}_T + 3\mathbf{A}_Z^\dagger \mathbf{A}_Z) - \frac{6}{5}M_1^2 g_1^2 - 6M_2^2 g_2^2, \\
16\pi^2 \frac{d\mathbf{m}_{\tilde{e}^c}^2}{dt} &= \left(2\mathbf{m}_{\tilde{e}^c}^2 + 4m_{H_1}^2 \right) \mathbf{Y}_e \mathbf{Y}_e^\dagger + 4\mathbf{Y}_e \mathbf{m}_{\tilde{L}}^2 \mathbf{Y}_e^\dagger + 2\mathbf{Y}_e \mathbf{Y}_e^\dagger \mathbf{m}_{\tilde{e}^c}^2 + 4\mathbf{A}_e \mathbf{A}_e^\dagger - \frac{24}{5}M_1^2 g_1^2, \\
16\pi^2 \frac{d\mathbf{m}_{\tilde{d}^c}^2}{dt} &= 2\mathbf{m}_{\tilde{d}^c}^2 (\mathbf{Y}_d \mathbf{Y}_d^\dagger + 2\mathbf{Y}_S \mathbf{Y}_S^\dagger + \mathbf{Y}_Z \mathbf{Y}_Z^\dagger) + 2(\mathbf{Y}_d \mathbf{Y}_d^\dagger + 2\mathbf{Y}_S \mathbf{Y}_S^\dagger + \mathbf{Y}_Z \mathbf{Y}_Z^\dagger) \mathbf{m}_{\tilde{d}^c}^2 \\
&\quad + 4 \left(\mathbf{Y}_d m_{H_1}^2 \mathbf{Y}_d^\dagger + \mathbf{Y}_d \mathbf{m}_{\tilde{Q}}^2 \mathbf{Y}_d^\dagger + 2\mathbf{Y}_S \mathbf{m}_{\tilde{d}^c}^2 \mathbf{Y}_S^\dagger + \mathbf{Y}_Z \mathbf{m}_{\tilde{L}}^2 \mathbf{Y}_Z^\dagger + 2\mathbf{Y}_S m_S^2 \mathbf{Y}_S^\dagger \right. \\
&\quad \left. + \mathbf{Y}_Z m_Z^2 \mathbf{Y}_Z^\dagger \right) + 4(\mathbf{A}_d \mathbf{A}_d^\dagger + 2\mathbf{A}_S \mathbf{A}_S^\dagger + \mathbf{A}_Z \mathbf{A}_Z^\dagger) - \frac{8}{15}M_1^2 g_1^2 - \frac{32}{3}M_3^2 g_3^2, \\
16\pi^2 \frac{d\mathbf{m}_{\tilde{u}^c}^2}{dt} &= \left(2\mathbf{m}_{\tilde{u}^c}^2 + 4m_{H_2}^2 \right) \mathbf{Y}_u \mathbf{Y}_u^\dagger + 4\mathbf{Y}_u \mathbf{m}_{\tilde{Q}}^2 \mathbf{Y}_u^\dagger + 2\mathbf{Y}_u \mathbf{Y}_u^\dagger \mathbf{m}_{\tilde{u}^c}^2 + 4\mathbf{A}_u \mathbf{A}_u^\dagger \\
&\quad - \frac{32}{15}M_1^2 g_1^2 - \frac{32}{3}M_3^2 g_3^2, \\
16\pi^2 \frac{d\mathbf{m}_{\tilde{Q}}^2}{dt} &= \left(\mathbf{m}_{\tilde{Q}}^2 + 2m_{H_2}^2 \right) \mathbf{Y}_u^\dagger \mathbf{Y}_u + \left(\mathbf{m}_{\tilde{Q}}^2 + 2m_{H_1}^2 \right) \mathbf{Y}_d^\dagger \mathbf{Y}_d + \left(\mathbf{Y}_u^\dagger \mathbf{Y}_u + \mathbf{Y}_d^\dagger \mathbf{Y}_d \right) \mathbf{m}_{\tilde{Q}}^2 \\
&\quad + 2\mathbf{Y}_u^\dagger \mathbf{m}_{\tilde{u}^c}^2 \mathbf{Y}_u + 2\mathbf{Y}_d^\dagger \mathbf{m}_{\tilde{d}^c}^2 \mathbf{Y}_d + 2\mathbf{A}_u^\dagger \mathbf{A}_u + 2\mathbf{A}_d^\dagger \mathbf{A}_d \\
&\quad - \frac{2}{15}M_1^2 g_1^2 - 6M_2^2 g_2^2 - \frac{32}{3}M_3^2 g_3^2. \tag{53}
\end{aligned}$$

The RGEs for the other soft-breaking masses are:

$$16\pi^2 \frac{dm_T^2}{dt} = 2 \left[m_T^2 (|\lambda_1|^2 + \text{Tr}(\mathbf{Y}_T^\dagger \mathbf{Y}_T)) + 2\text{Tr}(\mathbf{Y}_T^\dagger \mathbf{m}_{\tilde{L}}^2 \mathbf{Y}_T) + 2m_{H_1}^2 |\lambda_1|^2 \right]$$

$$\begin{aligned}
& +\text{Tr}(\mathbf{A}_T^\dagger \mathbf{A}_T) + |A_1|^2] - \frac{24}{5} M_1^2 g_1^2 - 16 M_2^2 g_2^2, \\
16\pi^2 \frac{dm_T^2}{dt} &= 2 \left(m_T^2 |\lambda_2|^2 + 2m_{H_2}^2 |\lambda_2|^2 + |A_2|^2 \right) - \frac{24}{5} M_1^2 g_1^2 - 16 M_2^2 g_2^2, \\
16\pi^2 \frac{dm_S^2}{dt} &= 2m_S^2 \text{Tr}(\mathbf{Y}_S^\dagger \mathbf{Y}_S) + 4 \left[\text{Tr}(\mathbf{Y}_S^\dagger \mathbf{m}_{d^c}^2 \mathbf{Y}_S) + \text{Tr}(\mathbf{A}_S^\dagger \mathbf{A}_S) \right] - \frac{32}{15} M_1^2 g_1^2 - \frac{80}{3} M_3^2 g_3^2, \\
16\pi^2 \frac{dm_{\bar{S}}^2}{dt} &= -\frac{32}{15} M_1^2 g_1^2 - \frac{80}{3} M_3^2 g_3^2, \\
16\pi^2 \frac{dm_Z^2}{dt} &= 2m_Z^2 \text{Tr}(\mathbf{Y}_Z^\dagger \mathbf{Y}_Z) + \left[\text{Tr}(\mathbf{Y}_Z^\dagger \mathbf{m}_{d^c}^2 \mathbf{Y}_Z) + \text{Tr}(\mathbf{Y}_Z^\star \mathbf{m}_L^{2T} \mathbf{Y}_Z^T) + \text{Tr}(\mathbf{A}_Z^\dagger \mathbf{A}_Z) \right] \\
&\quad - \frac{2}{15} M_1^2 g_1^2 - 6 M_2^2 g_2^2 - \frac{32}{3} M_3^2 g_3^2, \\
16\pi^2 \frac{dm_{\bar{Z}}^2}{dt} &= -\frac{2}{15} M_1^2 g_1^2 - 6 M_2^2 g_2^2 - \frac{32}{3} M_3^2 g_3^2, \\
16\pi^2 \frac{dm_{H_1}^2}{dt} &= 2m_{H_1}^2 \left[\text{Tr}(\mathbf{Y}_e \mathbf{Y}_e^\dagger) + 3\text{Tr}(\mathbf{Y}_d \mathbf{Y}_d^\dagger) + 6|\lambda_1|^2 \right] + 2 \left[3\text{Tr}(\mathbf{Y}_d^\dagger \mathbf{m}_{d^c}^2 \mathbf{Y}_d + \mathbf{Y}_d \mathbf{m}_{\bar{Q}}^2 \mathbf{Y}_d^\dagger) \right. \\
&\quad \left. + \text{Tr}(\mathbf{Y}_e \mathbf{m}_{\bar{L}}^2 \mathbf{Y}_e^\dagger + \mathbf{Y}_e^\dagger \mathbf{m}_{e^c}^2 \mathbf{Y}_e) \right] + 6|\lambda_1|^2 m_T^2 \\
&\quad + 2 \left[3\text{Tr}(\mathbf{A}_d \mathbf{A}_d^\dagger) + \text{Tr}(\mathbf{A}_e \mathbf{A}_e^\dagger) + 3|A_1|^2 \right] - \frac{6}{5} M_1^2 g_1^2 - 6 M_2^2 g_2^2, \\
16\pi^2 \frac{dm_{H_2}^2}{dt} &= 2m_{H_2}^2 \left[3\text{Tr}(\mathbf{Y}_u \mathbf{Y}_u^\dagger) + 6|\lambda_2|^2 \right] + 6\text{Tr}(\mathbf{Y}_u^\dagger \mathbf{m}_{u^c}^2 \mathbf{Y}_u + \mathbf{Y}_u \mathbf{m}_{\bar{Q}}^2 \mathbf{Y}_u^\dagger) \\
&\quad + 6|\lambda_2|^2 m_T^2 + 6 \left[\text{Tr}(\mathbf{A}_u \mathbf{A}_u^\dagger) + |A_2|^2 \right] - \frac{6}{5} M_1^2 g_1^2 - 6 M_2^2 g_2^2. \tag{54}
\end{aligned}$$

As for the soft-breaking trilinear coupling matrices we have:

$$\begin{aligned}
16\pi^2 \frac{d\mathbf{A}_T}{dt} &= \mathbf{A}_T \left[\mathbf{Y}_e^\dagger \mathbf{Y}_e + 9\mathbf{Y}_T^\dagger \mathbf{Y}_T + 3\mathbf{Y}_Z^\dagger \mathbf{Y}_Z + \text{Tr}(\mathbf{Y}_T^\dagger \mathbf{Y}_T) + |\lambda_1|^2 - \frac{9}{5} g_1^2 - 7g_2^2 \right] \\
&\quad + \left(\mathbf{Y}_e^T \mathbf{Y}_e^\star + 9\mathbf{Y}_T \mathbf{Y}_T^\dagger + 3\mathbf{Y}_Z^T \mathbf{Y}_Z^\star \right) \mathbf{A}_T + 6\mathbf{A}_Z^T \mathbf{Y}_Z^\star \mathbf{Y}_T \\
&\quad + 2\mathbf{Y}_T \left[3\mathbf{Y}_Z^\dagger \mathbf{A}_Z + \text{Tr}(\mathbf{Y}_T^\dagger \mathbf{A}_T) + \lambda_1^\star A_1 + \frac{9}{5} M_1 g_1^2 + 7M_2 g_2^2 \right], \\
16\pi^2 \frac{d\mathbf{A}_S}{dt} &= \mathbf{A}_S \left[12\mathbf{Y}_S^\dagger \mathbf{Y}_S + 2\mathbf{Y}_d^\star \mathbf{Y}_d^T + 2\mathbf{Y}_Z^\star \mathbf{Y}_Z^T + \text{Tr}(\mathbf{Y}_S^\dagger \mathbf{Y}_S) - \frac{4}{5} g_1^2 - 12g_3^2 \right] \\
&\quad + 2 \left(6\mathbf{Y}_S \mathbf{Y}_S^\dagger + \mathbf{Y}_d \mathbf{Y}_d^\dagger + \mathbf{Y}_Z \mathbf{Y}_Z^\dagger \right) \mathbf{A}_S + 4(\mathbf{A}_d \mathbf{Y}_d^\dagger + \mathbf{A}_Z \mathbf{Y}_Z^\dagger) \mathbf{Y}_S \\
&\quad + 2\mathbf{Y}_S \left[2\mathbf{Y}_d^\star \mathbf{A}_d^T + 2\mathbf{Y}_Z^\star \mathbf{A}_Z^T + \text{Tr}(\mathbf{Y}_S^\dagger \mathbf{A}_S) + \frac{4}{5} M_1 g_1^2 + 12M_2 g_3^2 \right], \\
16\pi^2 \frac{d\mathbf{A}_Z}{dt} &= \mathbf{A}_Z \left[\mathbf{Y}_e^\dagger \mathbf{Y}_e + 3\mathbf{Y}_T^\dagger \mathbf{Y}_T + 7\mathbf{Y}_Z^\dagger \mathbf{Y}_Z + \text{Tr}(\mathbf{Y}_Z^\dagger \mathbf{Y}_Z) - \frac{7}{15} g_1^2 - 3g_2^2 - \frac{16}{3} g_3^2 \right] \\
&\quad + 2 \left(2\mathbf{Y}_S \mathbf{Y}_S^\dagger + \mathbf{Y}_d \mathbf{Y}_d^\dagger + 2\mathbf{Y}_Z \mathbf{Y}_Z^\dagger \right) \mathbf{A}_Z + 6\mathbf{Y}_Z \mathbf{Y}_T^\dagger \mathbf{A}_T \\
&\quad + 2 \left[\mathbf{A}_d \mathbf{Y}_d^\dagger + 4\mathbf{A}_S \mathbf{Y}_S^\dagger + \frac{7}{15} M_1 g_1^2 + 3M_2 g_2^2 + \frac{16}{3} M_3 g_3^2 \right] \mathbf{Y}_Z, \\
16\pi^2 \frac{d\mathbf{A}_e}{dt} &= \mathbf{A}_e \left[5\mathbf{Y}_e^\dagger \mathbf{Y}_e + 3\mathbf{Y}_Z^\dagger \mathbf{Y}_Z + \text{Tr}(\mathbf{Y}_e \mathbf{Y}_e^\dagger + 3\mathbf{Y}_d \mathbf{Y}_d^\dagger) + 3|\lambda_1|^2 + 3\mathbf{Y}_T^\dagger \mathbf{Y}_T - \frac{9}{5} g_1^2 - 3g_2^2 \right]
\end{aligned}$$

$$\begin{aligned}
& +2\mathbf{Y}_e \left[2\mathbf{Y}_e^\dagger \mathbf{A}_e + \text{Tr}(\mathbf{A}_e \mathbf{Y}_e^\dagger + 3\mathbf{A}_d \mathbf{Y}_d^\dagger) + 3\lambda_1^* A_1 + 3\mathbf{Y}_T^\dagger \mathbf{A}_T + 3\mathbf{Y}_Z^\dagger \mathbf{A}_Z \right. \\
& \quad \left. + \frac{9}{5} M_1 g_1^2 + 3M_2 g_2^2 \right], \\
16\pi^2 \frac{d\mathbf{A}_d}{dt} &= \mathbf{A}_d \left[5\mathbf{Y}_d^\dagger \mathbf{Y}_d + \mathbf{Y}_u^\dagger \mathbf{Y}_u + \text{Tr}(\mathbf{Y}_e \mathbf{Y}_e^\dagger + 3\mathbf{Y}_d \mathbf{Y}_d^\dagger) + 3|\lambda_1|^2 - \frac{7}{15} g_1^2 - 3g_2^2 - \frac{16}{3} g_3^2 \right] \\
& + 2 \left(2\mathbf{Y}_S \mathbf{Y}_S^\dagger + \mathbf{Y}_Z \mathbf{Y}_Z^\dagger \right) \mathbf{A}_d + 4 \left(2\mathbf{A}_S \mathbf{Y}_S^\dagger + \mathbf{A}_Z \mathbf{Y}_Z^\dagger \right) \mathbf{Y}_d \\
& + 2\mathbf{Y}_d \left[2\mathbf{Y}_d^\dagger \mathbf{A}_d + \mathbf{Y}_u^\dagger \mathbf{A}_u + \text{Tr}(\mathbf{A}_e \mathbf{Y}_e^\dagger + 3\mathbf{A}_d \mathbf{Y}_d^\dagger) + 3\lambda_1^* A_1 \right. \\
& \quad \left. + \frac{7}{15} M_1 g_1^2 + 3M_2 g_2^2 + \frac{16}{3} M_3 g_3^2 \right], \\
16\pi^2 \frac{d\mathbf{A}_u}{dt} &= \mathbf{A}_u \left[5\mathbf{Y}_u^\dagger \mathbf{Y}_u + \mathbf{Y}_d^\dagger \mathbf{Y}_d + 3\text{Tr}(\mathbf{Y}_u \mathbf{Y}_u^\dagger) + 3|\lambda_2|^2 - \frac{13}{15} g_1^2 - 3g_2^2 - \frac{16}{3} g_3^2 \right] \\
& + 2\mathbf{Y}_u \left[2\mathbf{Y}_u^\dagger \mathbf{A}_u + \mathbf{Y}_d^\dagger \mathbf{A}_d + 3\text{Tr}(\mathbf{A}_u \mathbf{Y}_u^\dagger) + 3\lambda_2^* A_2 + \frac{13}{15} M_1 g_1^2 + 3M_2 g_2^2 + \frac{16}{3} M_3 g_3^2 \right], \\
16\pi^2 \frac{dA_1}{dt} &= A_1 \left[2\text{Tr}(\mathbf{Y}_e^\dagger \mathbf{Y}_e + 3\mathbf{Y}_d^\dagger \mathbf{Y}_d) + \text{Tr}(\mathbf{Y}_T^\dagger \mathbf{Y}_T) + 21|\lambda_1|^2 - \frac{9}{5} g_1^2 - 7g_2^2 \right] \\
& + 2\lambda_1 \left[\text{Tr}(\mathbf{Y}_T^\dagger \mathbf{A}_T) + 2\text{Tr}(\mathbf{Y}_e^\dagger \mathbf{A}_e + 3\mathbf{Y}_d^\dagger \mathbf{A}_d) + \frac{9}{5} M_1 g_1^2 + 7M_2 g_2^2 \right], \\
16\pi^2 \frac{dA_2}{dt} &= A_2 \left[6\text{Tr}(\mathbf{Y}_u^\dagger \mathbf{Y}_u) + 21|\lambda_2|^2 - \frac{9}{5} g_1^2 - 7g_2^2 \right] \\
& + 2\lambda_2 \left[6\text{Tr}(\mathbf{Y}_u^\dagger \mathbf{A}_u) + \frac{9}{5} M_1 g_1^2 + 7M_2 g_2^2 \right]. \tag{55}
\end{aligned}$$

Clearly, all the RGEs shown above are valid in both scenarios (A) and (B). In the former scenario, the condition $\mathbf{Y}_S = \mathbf{Y}_Z = 0$ at M_G ensures that Yukawa couplings $\mathbf{Y}_S, \mathbf{Y}_Z$ and the parameters $\mathbf{A}_S, \mathbf{A}_Z$ are not radiatively induced, therefore they can be simply switched off in the r.h.s of any RGEs. Beneath the mass scale M_T , we recover the RGEs of the MSSM by switching off $\mathbf{Y}_{T,S,Z}, \lambda_{1,2}, m_{T,\bar{T}}^2, m_{S,\bar{S}}^2, m_{Z,\bar{Z}}^2$ and $\mathbf{A}_{T,S,Z}, A_{1,2}$. For completeness, we report also the RGE of the $d = 5$ neutrino-operator Yukawa matrix \mathbf{Y}_ν valid below M_T in the MSSM [26]:

$$16\pi^2 \frac{d\mathbf{Y}_\nu}{dt} = \mathbf{Y}_\nu \left[-\frac{6}{5} g_1^2 - 6g_2^2 + 6\text{Tr}(\mathbf{Y}_u^\dagger \mathbf{Y}_u) \right] + \mathbf{Y}_\nu \mathbf{Y}_e^\dagger \mathbf{Y}_e + (\mathbf{Y}_e^\dagger \mathbf{Y}_e)^T \mathbf{Y}_\nu. \tag{56}$$

References

- [1] T. Toshito [SuperKamiokande Collaboration], Proceedings of 6th Rencontres de Moriond on Electroweak Interactions and Unified Theories (Les Arcs, France, 10-17 March 2001).
- [2] B. T. Cleveland *et al.* [Homestake Collaboration], *Astrophys. J.* **496**, 505 (1998);
J. N. Adurashitov *et al.* [SAGE Collaboration], astro-ph/0204245;
W. Hampel *et al.* [GALLEX Collaboration], *Phys. Lett. B* **447** (1999) 127;
T. Kirsten *et al.* [GNO Collaboration], in *Neutrino 2002*, 20th Int. Conf. on Neutrino Physics and Astrophysics (Munich, Germany, 2002), to appear in the Proceedings;
Y. Fukuda *et al.* [Kamiokande Collaboration], *Phys. Rev. Lett.* **77** (1996) 1683; hep-ex/0205075;
Q. R. Ahmad *et al.* [SNO Collaboration], *Phys. Rev. Lett.* **87** (2001) 071301; nucl-ex/0204008; nucl-ex/0204009.
- [3] B. Pontecorvo, *Sov. Phys. JETP* **7** (1958) 172 [*J. Exptl. Theor. Fiz.* **34** (1958) 247]; *Sov. Phys. JETP* **26** (1968) 984 [*Zh. Eksp. Teor. Fiz.* **53** (1967) 1717];
S. M. Bilenky and B. Pontecorvo, *Phys. Rep.* **41** (1978) 225;
Z. Maki, M. Nakagawa and S. Sakata, *Prog. Theor. Phys.* **28** (1962) 870.
- [4] L. Wolfenstein, *Phys. Rev. D* **17** (1978) 2369;
S. P. Mikheev and A. Y. Smirnov, *Sov. J. Nucl. Phys.* **42** (1985) 913 [*Yad. Fiz.* **42** (1985) 1441] ; *Nuovo Cim. C* **9** (1986) 17.
- [5] S. Weinberg, *Phys. Rev. Lett.* **43** (1979) 1566;
R. Barbieri, J. Ellis and M.K. Gaillard, *Phys. Lett. B* **90** (1980) 249;
E. Akhmedov, Z. Berezhiani and G. Senjanović, *Phys. Rev. Lett.* **69** (1992) 3013.
- [6] For recent analyses, see for example:
M. C. Gonzalez-Garcia, M. Maltoni, C. Pena-Garay and J. W. F. Valle, *Phys. Rev. D* **63** (2001) 033005;
P. I. Krastev and A. Y. Smirnov, *Phys. Rev. D* **65** (2002) 073022;
G. L. Fogli, E. Lisi, A. Marrone, D. Montanino and A. Palazzo, hep-ph/0206162;
V. Barger, D. Marfatia and B. Wood, hep-ph/0204253;
J. N. Bahcall, M. C. Gonzalez-Garcia and C. Pena-Garay, hep-ph/0204314;
P. C. de Holanda and A. Y. Smirnov, hep-ph/0205241.
- [7] D. E. Groom *et al.* [Particle Data Group Collaboration], *Eur. Phys. J. C* **15** (2000) 1.
- [8] L. M. Barkov *et al.*, Research Proposal for an experiment at PSI (1999). See also the talk by W. Ootani [MEGA Collaboration] at the The 3rd Workshop on "Neutrino Oscillations and their Origin" (NOON2001), Dec. 2001, ICRR, Univ. of Tokyo, Kashiwa, Japan; transparencies available at: <http://meg.psi.ch/>.
- [9] As reported by J. Ellis *et al.*, *Eur. Phys. C* **14**, 319 (2000).

- [10] S. T. Petcov, Sov. J. Nucl. Phys. **25** (1977) 340 [Yad. Fiz. **25** (1977) 641; **25**, 698 (E) (1977); **25**, 1336 (E) (1977)];
T. P. Cheng and L. F. Li, Phys. Rev. D **16** (1977) 1425;
S. M. Bilenky, S. T. Petcov and B. Pontecorvo, Phys. Lett. B **67** (1977) 309;
W. J. Marciano and A. I. Sanda, Phys. Lett. B **67** (1977) 303;
B. W. Lee and R. E. Shrock, Phys. Rev. D **16** (1977) 1444.
- [11] J. Ellis and D. V. Nanopoulos, Phys. Lett. **B110** (1982) 44.
For a recent development:
A. Brignole and A. Rossi, Nucl. Phys. **B587** (2000) 3.
- [12] Y. Nir and N. Seiberg, Phys. Lett. B **309** (1993) 337; *ibidem* Phys. Lett. B **365** (1995) 163;
M. Dine, R. G. Leigh and A. Kagan, Phys. Rev. D **48** (1993) 4269;
R. Barbieri, G. R. Dvali and L. J. Hall, Phys. Lett. B **377** (1996) 76;
E. Dudas, S. Pokorski and C. A. Savoy, Phys. Lett. B **369** (1996) 255;
E. Dudas, C. Grojean, S. Pokorski and C. A. Savoy, Nucl. Phys. B **481** (1996) 85;
A. Pomarol and A. Tommasini, Nucl. Phys. B **466** (1996) 3;
R. Barbieri and L. J. Hall, Nuovo Cim. A **110** (1997) 1 ;
R. Barbieri, L. J. Hall, S. Raby and A. Romanino, Nucl. Phys. B **493** (1997) 3;
R. Barbieri, L. J. Hall and A. Romanino, Phys. Lett. B **401** (1997) 47;
Z. Berezhiani, Phys. Lett. B **417** (1998) 287.
- [13] F. Borzumati and A. Masiero, Phys. Rev. Lett. **57**, 961 (1986);
F. Gabbiani and A. Masiero, Nucl. Phys. B **322** (1989) 235.
- [14] L. J. Hall, V. A. Kostelecky and S. Raby, Nucl. Phys. B **267** (1986) 415;
R. Barbieri and L. J. Hall, Phys. Lett. B **338** (1994) 212 ;
S. Dimopoulos and A. Pomarol, Phys. Lett. B **353** (1995) 222.
- [15] M. Gell-Mann, P. Ramond and R. Slansky, in *Supergravity*, eds. D. Freedman *et al.*, North-Holland, Amsterdam, 1979;
T. Yanagida, Prog. Th. Phys. B135 (1979) 66;
R. Mohapatra and G. Senjanović, Phys. Rev. Lett. **44** (1980) 912.
- [16] J. Hisano, T. Moroi, K. Tobe and M. Yamaguchi, Phys. Rev. D **53** (1996) 2442;
J. Hisano, T. Moroi, K. Tobe and M. Yamaguchi, Phys. Lett. B **391** (1997) 341 [Erratum-*ibid.* B **397** (1997) 357];
J. Hisano, D. Nomura and T. Yanagida, Phys. Lett. B **437** (1998) 351;
J. Hisano and D. Nomura, Phys. Rev. D **59** (1999) 116005;
J. Hisano and K. Tobe, Phys. Lett. B **510** (2001) 197;
J. A. Casas and A. Ibarra, Nucl. Phys. B **618** (2001) 171;
A. Kageyama, S. Kaneko, N. Shimoyama and M. Tanimoto, Phys. Lett. B **527** (2002) 206; Phys. Rev. D **65** (2002) 096010;
S. Lavignac, I. Masina and C. A. Savoy, Nucl. Phys. B **633** (2002) 139.

- [17] G. B. Gelmini and M. Roncadelli, Phys. Lett. B **99** (1981) 411.
- [18] J. Schechter and J. W. Valle Phys. Rev. D **25** (1982) 774;
K. Choi and A. Santamaria, Phys. Lett. B **267** (1991) 504.
- [19] T. P. Cheng and L. F. Li, Phys. Rev. D **22** (1980) 2860;
C. Wetterich, Nucl. Phys. B **187** (1981) 343.
See also R. N. Mohapatra and G. Senjanovic, Phys. Rev. D **23** (1981) 165.
For a recent review see e.g: M. Fukugita and T. Yanagida, “Physics of Neutrinos”, in
“Physics and Astrophysics of Neutrinos”, p. 56, Ed. by M. Fukugita and A. Suzuki,
Tokyo, Japan: Springer (1994).
- [20] E. Ma and U. Sarkar, Phys. Rev. Lett. **80** (1998) 5716.
- [21] R. Foot, H. Lew, X. G. He and G. C. Joshi, Z. Phys. C **44** (1989) 441;
E. Ma, Phys. Rev. Lett. **81** (1998) 1171;
B. Brahmachari, E. Ma and U. Sarkar, Phys. Lett. B **520** (2001) 152;
B. Brahmachari, Phys. Rev. D **65** (2002) 067502.
- [22] T. Hambye, E. Ma and U. Sarkar, Nucl. Phys. B **602** (2001) 23.
- [23] S. Davidson and A. Ibarra, JHEP **0109** (2001) 013.
- [24] H. Georgi and C. Jarlskog, Phys. Lett. B **86** (1979) 297.
J. A. Harvey, P. Ramond and D. B. Reiss, Phys. Lett. B **92** (1980) 309.
For more recent works, see for example:
K. S. Babu and S. M. Barr, Phys. Rev. D **56** (1997) 2614;
Z. Berezhiani and A. Rossi, JHEP **9903** (1999) 002;
Z. Berezhiani and A. Rossi, Nucl. Phys. B **594** (2001) 113, and references therein.
- [25] S. Dimopoulos and H. Georgi, Nucl. Phys. B **193** (1981) 150;
N. Sakai, Z. Phys. C **11** (1981) 153;
E. Witten, Nucl. Phys. B **188** (1981) 513.
- [26] P. Chankowski and Z. Pluciennik, Phys. Lett. B **316** (1993) 312;
C.N. Leung, K.S. Babu and J. Pantaleone, *ibid.* B **319** (1993) 191;
- [27] J. Ellis and S. Lola, Phys. Lett. B **458** (1999) 310;
N. Haba and N. Okamura, Prog. Theor. Phys. **103** (2000) 367;
J.A. Casas, J.R. Espinosa, A. Ibarra and I. Navarro, Nucl. Phys. B **573** (2000) 652.
- [28] M. Apollonio *et al.* [CHOOZ Collaboration], Phys. Lett. B **466** (1999) 415.
- [29] F. Gabbiani *et al.*, Nucl. Phys. B **477** (1996) 321;
M. Ciuchini *et al.*, JHEP **9810** (1998) 008
- [30] N. K. Falck, Z. Phys. C **30** (1986) 247.